

Robust regression with compositional covariates

ADITYA K. MISHRA*, CHRISTIAN L. MÜLLER

Center for Computational Mathematics, Flatiron Institute, 162 5th Avenue, NY 10010

amishra@flatironinstitute.org

SUMMARY

Many biological high-throughput data sets, such as targeted amplicon-based and metagenomic sequencing data, are compositional in nature. A common exploratory data analysis task is to infer statistical associations between the high-dimensional microbial compositions and habitat- or host-related covariates. We propose a general robust statistical regression framework, **RobRegCC** (Robust Regression with Compositional Covariates), which extends the linear log-contrast model by a mean shift formulation for capturing outliers. **RobRegCC** includes sparsity-promoting convex and non-convex penalties for parsimonious model estimation, a data-driven robust initialization procedure, and a novel robust cross-validation model selection scheme. We show **RobRegCC**'s ability to perform simultaneous sparse log-contrast regression and outlier detection over a wide range of simulation settings and provide theoretical non-asymptotic guarantees for the underlying estimators. To demonstrate the seamless applicability of the workflow on real data, we consider a gut microbiome data set from HIV patients and infer robust associations between a sparse set of microbial species and host immune response from soluble CD14 measurements. All experiments are fully reproducible and available on GitHub at <https://github.com/amishra-stats/robregcc>.

*To whom correspondence should be addressed.

Key words: Compositional data; Microbiome; Robust regression; Mean shift; Sparsity; non-convexity

1. INTRODUCTION

Many scientific data measurements are compositional in nature. Prominent examples include chemical composition measurements of rocks and sediments in geology and relative abundances of sequencing reads in microbial ecology. For instances, targeted amplicon sequencing (TAS) and metagenomic profiling provides genomic survey data of microbial communities in their natural habitat, ranging from marine ecosystems to the human gut (Huttenhower *and others*, 2012; Thompson *and others*, 2017; Sunagawa *and others*, 2015; McDonald *and others*, 2018). These microbiome surveys typically comprise sparse relative (or compositional) counts of operational taxonomic units (OTUs) or amplicon sequence variants (ASVs) (Callahan *and others*, 2017; Edgar, 2016) and are often accompanied by measurements of additional covariates that characterize the underlying habitat or the phenotypic status of the host.

An important step in exploratory microbiome data analysis is the inference of parsimonious and robust statistical relationships between the microbial compositions and habitat- or host-specific measurements. Standard linear regression modeling can, however, not be applied in this context because the microbial count data only carry relative or compositional information. Several regression techniques have been introduced to handle compositional data, including Dirichlet multinomial mixture modeling (Holmes *and others*, 2012) and kernel penalized regression (Randolph *and others*, 2018). A popular approach to regression modeling with compositional covariates is log-contrast regression, put forward by Aitchison and Bacon-Shone (1984) in the context of experiments with mixtures. In the linear log-contrast model, the continuous response is expressed as linear combination of log-transformed compositions subject to a zero-sum constraint on the regression vector. This model allows the intuitive interpretation of the response as a linear combination of log-ratios of the original compositions. An alternative equivalent low-dimensional

approach considers linear regression after applying an isometric log-ratio (ilr) transform to the compositions (Hron *and others*, 2012).

For microbiome data analysis, the linear log-contrast model has been brought to the high-dimensional setting via regularization, e.g. via ℓ_1 penalization (Lin *and others*, 2014) or more general structured sparsity approaches (Shi *and others*, 2016; Wang and Zhao, 2017; Sun *and others*, 2018). A related approach is the selection of balance (selbal) approach (Rivera-Pinto *and others*, 2018) which performs sparse greedy covariate selection on ilr transformed variables. While these approaches can lead to parsimonious models linking (microbial) compositions to responses of interest, they are sensitive to outliers or high-leveraged data points in the response.

In this contribution, we alleviate these shortcomings by introducing **Robust** log-contrast **Regression** estimators with **Compositional Covariates** (RobRegCC), a novel robust regression modeling framework for compositional data. Figure 1 shows the general RobRegCC workflow.

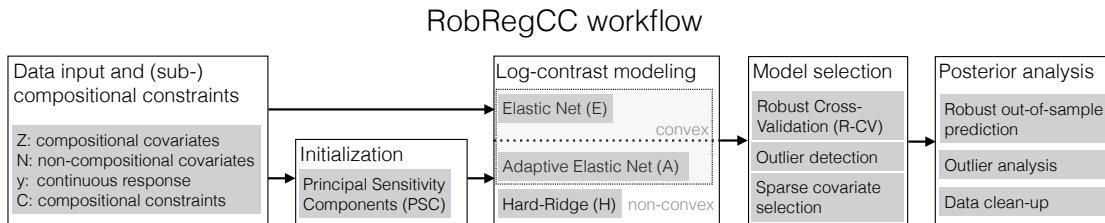


Figure 1. The RobRegCC workflow for robust regression with compositional covariates.

RobRegCC integrates a mean shift formulation in linear log-contrast regression which enables the modeling of outliers in the response variable. The approach achieves parsimonious model identification, i.e., simultaneous outlier detection and variable selection, through the integration of sparsity-promoting convex and non-convex regularizers. RobRegCC includes three different penalization approaches, the standard Elastic Net(E) penalty, a novel adaptive Elastic Net(A) penalty, and a non-convex hard-ridge (H) penalty, resulting in a family of robust

estimators. We derive theoretical guarantees for these estimators in the non-asymptotic setting. The latter two estimation procedures require initial parameter estimates which we provide via principal sensitivity component (PSC) analysis (Peña and Yohai, 1999), adapted to the compositional setting. We formulate the associated (non-)convex optimization problems using an augmented Lagrangian framework and present an iterative thresholding/proximal algorithm for efficient numerical minimization. RobRegCC also includes novel robust model selection and robust out-of-sample prediction measures which may be of independent interest. For model selection, we put forward a robust cross-validation (R-CV) scheme which computes test sample error on “clean” leave-out data using a specifically tailored robust test statistics. The same statistic is also used to perform robust out-of-sample prediction. All presented simulation and real-world experiments and computations are available in a reproducible workflow on GitHub at <https://github.com/amishra-stats/robregcc>. RobRegCC is available on CRAN at <https://CRAN.R-project.org/package=robregcc>.

2. ROBUST LOG-CONTRAST REGRESSION FOR COMPOSITIONAL DATA

High-throughput next-generation sequencing techniques typically provide read count data of the form $\mathbf{D} = [\mathbf{d}_1, \dots, \mathbf{d}_n]^T \in \mathbb{R}^{n \times p}$, comprising n observations of a p -dimensional vector of read counts. The counts correspond, for instance, to the estimated number of OTUs, ASVs, or genes in a biological sample. Due to experimental limitations, the read counts only carry relative or proportional information and do not represent absolute abundances. One way to normalize these count data is to divide each sample by its total sum, resulting in a matrix $\mathbf{W} = [\mathbf{w}_1, \dots, \mathbf{w}_n]^T \in \mathbb{R}^{n \times p}$ where each $\mathbf{w}_i = \mathbf{d}_i / \mathbf{1}_p^T \mathbf{d}_i$ represents a p -dimensional vector of proportions or compositions. Prior to the normalization, any zero count is replaced by a constant pseudo-count (Aitchison, 1982) or a small random count generated from an appropriate probability distribution (Friedman and Alm, 2012). Any compositional vector \mathbf{w}_i is thus constraint to the $(p - 1)$ -dimensional

simplex $\mathbf{S}^{(p-1)} = \{[s_1, \dots, s_p]^T : 0 < s_k \leq 1, \sum_{k=1}^p s_k = 1\}$. The problem of interest is to find linear associations between the measured compositions \mathbf{W} and a continuous response or outcome variable of interest $\mathbf{y} = [y_1, \dots, y_n]^T \in \mathbb{R}^n$ that has been jointly collected with the relative abundance data. Aitchison and Bacon-Shone (1984) provide a useful framework to model such associations via log-contrast regression.

2.1 The standard log-contrast regression model

The principle idea of log-contrast regression is to model the outcome \mathbf{y} as linear combination of log-ratios derived from the compositional covariate data \mathbf{W} . A common transform is the additive log-ratio (alr) transform (Aitchison, 1982) which requires the choice of a reference. When considering the k th predictor as reference, the alr-transformed data are $\mathbf{U} = [\mathbf{u}_1, \dots, \mathbf{u}_n]^T$, where $\mathbf{u}_i = [u_{i1}, \dots, u_{ip}]$ with $u_{ij} = \log(w_{ij}/w_{ik})$. The log-contrast regression model is written as

$$y_i = \mathbf{u}_{i,-k} \mathbf{b}_{-k} + \epsilon_i, \quad i = 1, \dots, n \quad (2.1)$$

where $\mathbf{b} = [b_1 \dots b_p]^T$ is the coefficient vector, and $\boldsymbol{\epsilon} = [\epsilon_1 \dots \epsilon_n] \in \mathbb{R}^n$ is independent and identically distributed (IID) noise with mean $\mathbb{E}(\epsilon_i) = 0$ and variance $\text{Var}(\epsilon_i) = \sigma^2$. The symbol $-k$ denotes the exclusion of k th entries in \mathbf{u}_i and \mathbf{b} . A major drawback of model (2.1) is its loss of permutation invariance due to the choice of a reference (Aitchison, 1982). By expressing $b_k = -\sum_{i \neq k} b_i$, we can reformulate model (2.1) into a symmetric permutation-invariant form as

$$y_i = \mathbf{z}_i^T \mathbf{b} + \epsilon_i, \quad \mathbf{1}_p^T \mathbf{b} = 0, \quad i = 1, \dots, n, \quad (2.2)$$

where $\mathbf{z}_i = [z_{i1} \dots z_{ip}]^T$ are log-transformed predictors with $z_{ij} = \log(w_{ij})$ (Aitchison and Bacon-Shone, 1984). The linear constraint in (2.2) ensures that, after model fitting, the response can be equivalently expressed as linear combinations of log-ratios of the original compositions (Aitchison, 2003; Sun *and others*, 2018; Bates and Tibshirani, 2018; Combettes and Müller, 2020). The model also ensures subcompositional coherence, a key principle in compositional data analysis. This

principle states that the analysis should be coherent even if we had only selected subcompositions out of the full compositions, or if the analyzed compositions are only parts of larger compositions containing other parts.

When additional m non-compositional covariates $\mathbf{N} \in \mathbb{R}^{n \times m}$, such as habitat and host-associated factors or other control variables are available, we can extend the linear log-contrast model to

$$\mathbf{y} = \mathbf{Z}\mathbf{b} + \mathbf{N}\mathbf{a} + \boldsymbol{\epsilon}, \quad \mathbf{1}_p^\top \mathbf{b} = 0, \quad (2.3)$$

where $\mathbf{Z} = [\mathbf{z}_1, \dots, \mathbf{z}_n]^\top$, $\mathbf{b} \in \mathbb{R}^p$ is the coefficient vector for the compositional covariates, and $\mathbf{a} \in \mathbb{R}^m$ is the coefficient vector for all non-compositional variables, respectively. This model also allows to include an unconstrained intercept in the linear log-contrast model by taking the first column of \mathbf{N} to be $\mathbf{1}_n$, the $n \times 1$ vector of ones.

The zero-sum constraint in (2.3) can be generalized when grouping information about the predictors is available. In the microbiome context, each predictor can be associated with taxonomic or phylogenetic information, typically encoded in a taxonomic or phylogenetic tree $\mathcal{T}_{K,p}$ with p leaves and K levels. Following Shi *and others* (2016), we can include this information in (2.3) via a linear equality constraint. For instance, when analyzing microbiome data at a fixed (taxonomic or phylogenetic) level of the tree, e.g., at the phylum level, this level induces a grouping of the p taxa into k disjoint sets with column index set \mathbb{A}_r such that $|\mathbb{A}_r| = p_r$ for $r = 1, \dots, k$ and $\sum_{r=1}^k p_r = p$. Each set represents the taxa in the respective phylum. If the goal of the analysis is to be subcompositionally coherent with respect to the phylum groups, we can define the subcomposition matrix \mathbf{C}_s :

$$\mathbf{C}_s^\top = [\mathbf{c}_1 \quad \mathbf{c}_2 \quad \mathbf{c}_3 \quad \dots \quad \mathbf{c}_k]^\top = \begin{bmatrix} \mathbf{1}_{p_1}^\top & \mathbf{0} & \dots & \mathbf{0} \\ \mathbf{0} & \mathbf{1}_{p_2}^\top & \dots & \mathbf{0} \\ \vdots & \vdots & \ddots & \vdots \\ \mathbf{0} & \mathbf{0} & \dots & \mathbf{1}_{p_k}^\top \end{bmatrix}_{k \times p}, \quad (2.4)$$

where \mathbf{c}_j accounts for the composition in the subgroup with index set \mathbb{A}_j such that $(\mathbf{c}_j)_{\mathbb{A}_j} = \mathbf{1}_{p_j}$.

The model in (2.3) can thus be generalized by including the subcomposition matrix \mathbf{C}_s :

$$\mathbf{y} = \mathbf{Z}\mathbf{b} + \mathbf{N}\mathbf{a} + \boldsymbol{\epsilon} = \sum_{r=1}^k \mathbf{Z}_{\mathbb{A}_r} \mathbf{b}_{\mathbb{A}_r} + \mathbf{N}\mathbf{a} + \boldsymbol{\epsilon}, \quad \text{s.t.} \quad \mathbf{C}_s^T \mathbf{b} = \mathbf{0}, \quad (2.5)$$

where $\{\mathbf{Z}_{\mathbb{A}_r}, \mathbf{b}_{\mathbb{A}_r}\}$ are the covariates and unknown coefficients corresponding to the r th sub-group.

The model in (2.3) is a special case of model (2.5) with $\mathbf{C}_s = \mathbf{1}_p$.

2.2 Robust log-contrast regression model

Many biological datasets, including microbiome profiling data, contain outliers or other forms of data corruptions that can hamper statistical estimation. For example, the extended log-contrast model in (2.5) assumes errors $\boldsymbol{\epsilon}$ to be well behaved, i.e., free from outliers in $[\mathbf{y}, \mathbf{Z}, \mathbf{N}]$. Following earlier work for wavelet estimation in partial linear model (Antoniadis, 2007; Gannaz, 2007) and linear regression (She and Owen, 2011; Lee *and others*, 2012; Nasrabadi *and others*, 2011), we propose to extend the log-contrast model in (2.5) with a mean shift vector $\boldsymbol{\gamma} = [\gamma_1, \dots, \gamma_n]^T$, accounting for the grossly corrupted observations in y , resulting in the model

$$\mathbf{y} = \mathbf{Z}\mathbf{b} + \mathbf{N}\mathbf{a} + \boldsymbol{\gamma} + \boldsymbol{\epsilon}, \quad \text{s.t.} \quad \mathbf{C}_s^T \mathbf{b} = \mathbf{0}. \quad (2.6)$$

The support set $\mathcal{J}(\boldsymbol{\gamma})$ of the vector $\boldsymbol{\gamma}$ can thus capture potential outliers in the response y . By fusing the compositional and non-compositional covariates into the general design matrix $\mathbf{X} = [\mathbf{Z} \ \mathbf{N}]$, we can denote the corresponding model coefficients by $\boldsymbol{\beta} = (\mathbf{b} \ \mathbf{a}) \in \mathbb{R}^p$. Augmenting the linear constraint matrix \mathbf{C}_s by a $k \times m$ zero-matrix, denoted by $\mathbf{C} = [\mathbf{C}_s^T \ \mathbf{0}_{k \times m}]^T$, the model in (2.6) simplifies to

$$\mathbf{y} = \mathbf{X}\boldsymbol{\beta} + \boldsymbol{\gamma} + \boldsymbol{\epsilon}, \quad \text{s.t.} \quad \mathbf{C}^T \boldsymbol{\beta} = \mathbf{0}. \quad (2.7)$$

This model forms the basis for the **Robust** log-contrast **Regression** estimators with **Compositional Covariates** (RobRegCC), considered in the remainder of the paper.

2.3 Regularization for parameter estimation

As the RobRegCC model in (2.7) is over-specified even in the low-dimensional setting, comprising $(p+m+n-k)$ unknown parameters, we introduce a family of regularized estimators using sparsity-inducing penalties. The proposed class of estimators for the parameters $(\boldsymbol{\gamma}, \boldsymbol{\beta})$ are associated with the following general optimization problem:

$$(\widehat{\boldsymbol{\gamma}}, \widehat{\boldsymbol{\beta}}) \equiv \arg \min_{\boldsymbol{\gamma}, \boldsymbol{\beta}} \left\{ \frac{1}{2n} \|\mathbf{y} - \mathbf{X}\boldsymbol{\beta} - \boldsymbol{\gamma}\|_2^2 + P_{\lambda_1}^1(\boldsymbol{\gamma}) + P_{\lambda_2}^2(\boldsymbol{\beta}) \right\} \quad \text{s.t.} \quad \mathbf{C}^T \boldsymbol{\beta} = \mathbf{0}, \quad (2.8)$$

where $P_{\lambda_1}^1(\boldsymbol{\gamma})$ and $P_{\lambda_2}^2(\boldsymbol{\beta})$ are sparsity-inducing regularizers with tuning parameters λ_1 and λ_2 , respectively. The regularization framework involves solving the optimization problem (2.8) over a grid of tuning parameters $\{\lambda_1, \lambda_2\}$. Our theoretical results (see Theorem 4.1 in Section 4) show that optimal tuning can be achieved by setting $\lambda_1 = A\sigma(\log(en))^{1/2}$ and $\lambda_2 = A\sigma(\log(ep))^{1/2}$ for some constant A . This motivates the introduction of a single tuning parameter λ and expressing $\lambda_1 = k_1\lambda$ and $\lambda_2 = k_2\lambda$ where $k_1 = \sqrt{\log(en)}$ and $k_2 = \sqrt{\log(ep)}$.

Normalizing the ℓ_2 -norm of the columns of \mathbf{X} to \sqrt{n} , scaling the mean shift vector $\boldsymbol{\gamma}$ by the factor \sqrt{n} , and concatenating the unknowns into $\boldsymbol{\delta} = [\delta_1, \dots, \delta_{n+p}]^T = [\boldsymbol{\gamma}^T \boldsymbol{\beta}^T]^T$ leads to a compact reformulation of (2.8) of the form:

$$(\widehat{\boldsymbol{\gamma}}, \widehat{\boldsymbol{\beta}}) \equiv \arg \min_{\boldsymbol{\gamma}, \boldsymbol{\beta}} \left\{ \frac{1}{2n} \|\mathbf{y} - \mathbf{X}\boldsymbol{\beta} - \sqrt{n}\boldsymbol{\gamma}\|_2^2 + P_\lambda(\boldsymbol{\delta}) \right\} \quad \text{s.t.} \quad \mathbf{C}^T \boldsymbol{\beta} = \mathbf{0}, \quad (2.9)$$

with $P_\lambda(\boldsymbol{\delta}) = P_{\lambda_1}^1(\boldsymbol{\gamma}) + P_{\lambda_2}^2(\boldsymbol{\beta})$.

We focus, in theory and practice, on three different choices for the penalty function $P_\lambda(\boldsymbol{\delta})$:

$$\text{I) } P_\lambda^H(\boldsymbol{\delta}; \alpha) = \alpha\lambda^2 \sum_{i=1}^{n+p} \kappa_i^2 \|\delta_i\|_0 / 2 + (1 - \alpha)\lambda \|\boldsymbol{\delta}\|_2^2 / 2,$$

$$\text{II) } P_\lambda^E(\boldsymbol{\delta}; \alpha) = \alpha\lambda \|\boldsymbol{\kappa} \circ \boldsymbol{\delta}\|_1 + (1 - \alpha)\lambda \|\boldsymbol{\delta}\|_2^2 / 2,$$

$$\text{III) } P_\lambda^A(\boldsymbol{\delta}; \alpha, \mathbf{w}) = \alpha\lambda \|\boldsymbol{\kappa} \circ \mathbf{w} \circ \boldsymbol{\delta}\|_1 + (1 - \alpha)\lambda \|\boldsymbol{\delta}\|_2^2 / 2.$$

The vector $\boldsymbol{\kappa} = [\kappa_1, \dots, \kappa_{n+p}]^T = [k_1 \mathbf{1}_n^T \quad k_2 \mathbf{1}_p^T]^T$ represents the multiplying factors to each model parameter in $\boldsymbol{\delta}$, \mathbf{w} a vector of non-negative weights, and $\alpha \in [0, 1]$ the mixing weight between the

sparsity-inducing ℓ_0/ℓ_1 -norm and the ℓ_2 -norm, respectively. The symbol \circ denotes the element-wise product. Penalty function I comprises a mixture of the non-convex ℓ_0 “norm” and ridge (or Tikhonov) regularization via the squared ℓ_2 -norm. Following She and Owen (2011), we refer to this penalty as the hard-ridge penalty P^H . Penalty II is a convex relaxation of penalty I, the so-called “Elastic-Net” penalty (Zou and Hastie, 2005) as mixture of ℓ_1 -norm and squared ℓ_2 -norm and is denoted by P^E . Penalty III augments penalty II by a non-negative weight vector \mathbf{w} in the ℓ_1 -norm leading to a weighted or “adaptive” penalty P^A , similar to the adaptive lasso (Zou, 2006). This convex penalty is novel in the context of mean shift estimation and requires the construction of appropriate weights \mathbf{w} via a robust data-driven initialization procedure (see Section 3.2).

REMARK 2.1 The choice of the penalty function determines the properties of the corresponding robust estimator. In the low-dimensional setting, Antoniadis (2007) and Gannaz (2007) showed equivalence between Huber’s M-estimator and the mean shift model with ℓ_1 norm penalization. In robust linear regression, this model, even with added ℓ_2 regularization (i.e., the P^E penalty), is prone to “masking” and “swapping” effects due to leveraged outliers (She and Owen, 2011). Our simulation experiments (see Section 3) also confirm this behavior in log-contrast regression. To alleviate this shortcoming RobRegCC includes the non-convex hard-ridge penalty function P^H She and Owen (2011) and the convex adaptive penalty function P^A which inherits the statistical strength of P^H while simultaneously simplifying computation.

3. A UNIFYING COMPUTATIONAL FRAMEWORK FOR ROBUST LOG-CONTRAST REGRESSION

The computational framework (see Figure 1) for parameter estimation of the robust log-contrast regression model in (2.7) comprises three parts: (i) a novel robust initialization procedure that is instrumental when penalty functions I or III are used, (ii) a general algorithm for solving the

optimization problem in (2.9) that can encompass any of the introduced penalty functions, and (iii) a new robust cross-validation-based (R-CV) model selection strategy specifically tailored to robust estimation.

3.1 A general optimization algorithm

Our algorithmic framework can handle the optimization problem in (2.9) with any of the penalty functions I-III. While specialized optimization strategies are available for the convex problem instances, (see, e.g., Antoniadis and Fan (2001); Combettes and Pesquet (2011); She and Owen (2011); Combettes and Pesquet (2012); Briceño-Arias and Rivera (2018)), we present an general iterative thresholding algorithm, derived from an augmented Lagrangian formulation, that can encompass all penalty functions.

A fundamental building block for the proposed algorithm is the use of the proximity or thresholding operator $\Theta(\cdot)$ associated with a penalty function $P(\cdot)$:

$$\Theta(t) = \arg \min_{\theta} \frac{1}{2} \|t - \theta\|^2 + P(\theta).$$

For any scalar a , the soft thresholding operator is defined as $\Theta_{\lambda}^S(a) = \text{sign}(a)(|a| - \lambda)_+$, and the hard threshold operator is $\Theta_{\lambda}^H(a) = a1_{|a| > \lambda}$. Table 1 summarizes the parameterized scalar thresholding operators, associated with the penalty functions I-III (see also Antoniadis and Fan (2001); She and Owen (2011); Combettes and Pesquet (2011)). Note that for vector-valued input to the penalty functions, the thresholding operators are applied element-wise.

Table 1. Penalty function and corresponding thresholding/proximity operator.

Case	$P_{\lambda}(\theta; \alpha, w)$	$\Theta_{\lambda}(t)$
I	$\alpha^2 \lambda^2 \kappa^2 \ \theta\ _0 / 2 + (1 - \alpha) \lambda \ \theta\ _2^2 / 2$	$\Theta_c^H\left(\frac{t}{1 + \lambda(1 - \alpha)}\right)$ with $c = \frac{\alpha \lambda \kappa}{\sqrt{1 + \lambda(1 - \alpha)}}$
II	$\alpha \lambda \ \kappa \circ \theta\ _1 + (1 - \alpha) \lambda \ \theta\ _2^2 / 2$	$\frac{1}{1 + \lambda(1 - \alpha)} \Theta_{\alpha \lambda \kappa}^S(t)$
III	$\alpha \lambda \ \kappa \circ w \circ \theta\ _1 + (1 - \alpha) \lambda \ \theta\ _2^2 / 2$	$\frac{1}{1 + \lambda(1 - \alpha)} \Theta_{w \alpha \lambda \kappa}^S(t)$

In the optimization problem in (2.9), the linear constraint $\mathbf{C}^T \boldsymbol{\beta} = \mathbf{0}$ implies $\boldsymbol{\beta} = \mathbf{P}_{\mathbf{C}}^\perp \boldsymbol{\theta}$ for any $\boldsymbol{\theta} \in \mathbb{R}^p$, where $\mathbf{P}_{\mathbf{C}}^\perp$ is the orthogonal complement of the projection matrix onto subspace \mathbf{C} . We can thus reformulate the optimization problem in (2.9) as

$$(\hat{\boldsymbol{\theta}}, \hat{\boldsymbol{\gamma}}) \equiv \arg \min_{\boldsymbol{\theta}, \boldsymbol{\gamma}} \left\{ f_\lambda(\boldsymbol{\theta}, \boldsymbol{\gamma}) \right\} \quad \text{s.t. } \mathbf{C}^T \boldsymbol{\theta} = \mathbf{0}, \quad (3.10)$$

where $f_\lambda(\boldsymbol{\theta}, \boldsymbol{\gamma}) = \frac{1}{2n} \|\mathbf{y} - \mathbf{X} \mathbf{P}_{\mathbf{C}}^\perp \boldsymbol{\theta} - \sqrt{n} \boldsymbol{\gamma}\|_2^2 + P_{\lambda_1}^1(\boldsymbol{\gamma}) + P_{\lambda_2}^2(\boldsymbol{\theta})$. We solve the constraint optimization problem in (3.10) using an augmented Lagrangian approach. The standard augmented Lagrangian for the problem reads

$$L_{\mu, \lambda}(\boldsymbol{\theta}, \boldsymbol{\gamma}, \boldsymbol{\zeta}) = f_\lambda(\boldsymbol{\theta}, \boldsymbol{\gamma}) + \boldsymbol{\zeta}^T \mathbf{C}^T \boldsymbol{\theta} + \frac{\mu}{2} \|\mathbf{C}^T \boldsymbol{\theta}\|_2^2$$

where $\boldsymbol{\zeta} \in \mathbb{R}^k$ are the Lagrange multipliers and $\mu > 0$ is a regularization parameter. By reparameterizing $\boldsymbol{\eta} = \boldsymbol{\zeta}/\mu$ and completing the ‘‘square’’, the augmented Lagrangian simplifies to $L_{\mu, \lambda}(\boldsymbol{\theta}, \boldsymbol{\gamma}, \boldsymbol{\eta}) = f_\lambda(\boldsymbol{\theta}, \boldsymbol{\gamma}) + \frac{1}{2} \|\mathbf{C}^T \boldsymbol{\theta} + \boldsymbol{\eta}\|_2^2$.

We consider the dual descent approach for solving the associated optimization problem which iterates between

$$\text{Primal update: } (\boldsymbol{\theta}^{(i+1)}, \boldsymbol{\gamma}^{(i+1)}) \equiv \arg \min_{\boldsymbol{\theta}, \boldsymbol{\gamma}} \left\{ L_{\mu, \lambda}(\boldsymbol{\theta}, \boldsymbol{\gamma}, \boldsymbol{\eta}^{(i)}) \right\},$$

$$\text{Dual update: } \boldsymbol{\eta}^{(i+1)} = \boldsymbol{\eta}^{(i)} + \mathbf{C}^T \boldsymbol{\theta}^{(i+1)},$$

until certain convergence criteria are met. The primal update requires solving an unconstrained optimization problem for fixed Lagrange multipliers $\boldsymbol{\eta}^{(i)}$. By grouping all terms in the Lagrangian appropriately, we can rewrite this subproblem in standard form

$$\tilde{\boldsymbol{\theta}}^{(i+1)} \equiv \arg \min_{\tilde{\boldsymbol{\theta}}} \left\{ \frac{1}{2n} \|\tilde{\mathbf{y}} - \tilde{\mathbf{X}} \tilde{\boldsymbol{\theta}}\|_2^2 + P_\lambda(\tilde{\boldsymbol{\theta}}) \right\}, \quad (3.11)$$

where

$$\tilde{\mathbf{y}} = \begin{bmatrix} \mathbf{y} \\ -\sqrt{n} \boldsymbol{\eta}^{(i)} \end{bmatrix}, \quad \tilde{\boldsymbol{\theta}} = \begin{bmatrix} \boldsymbol{\theta} \\ \boldsymbol{\gamma} \end{bmatrix}, \quad \text{and} \quad \tilde{\mathbf{X}} = \begin{bmatrix} \mathbf{X} \mathbf{P}_{\mathbf{C}}^\perp & \sqrt{n} \mathbf{I} \\ \sqrt{n} \mathbf{C}^T & \mathbf{0} \end{bmatrix}.$$

For the penalty functions I-III, this problem formulation is amenable to iterative shrinkage/thresholding algorithms (ISTA) (see, e.g., Daubechies *and others* (2004); Combettes and Pesquet (2011)) or, equivalently, to the thresholding-based iterative selection procedure (TISP) (She, 2009). Convergence guarantees, however, depend on the specific properties of the penalty function. ISTA algorithms comprise a (forward) gradient step and a (backward) proximal/thresholding step. To solve the primal update at the $(i + 1)$ th stage for the objective in (3.11), the $(j + 1)$ th iteration in ISTA reads

$$\tilde{\boldsymbol{\theta}}^{(i,j+1)} = \Theta_\lambda \left[\tilde{\boldsymbol{\theta}}^{(i,j)} - \frac{1}{nk_0} \tilde{\mathbf{X}}^\top (\tilde{\mathbf{y}} - \tilde{\mathbf{X}} \tilde{\boldsymbol{\theta}}^{(i,j)}) \right], \quad (3.12)$$

where $\Theta_\lambda[\cdot]$ is the thresholding operator corresponding to the considered penalty function (see Table 1). The operator is applied element-wise to the entries of the vectors. The iterative algorithm is stopped when a prescribed convergence criterion on the consecutive iterates is reached. To ensure monotone decrease in the objective function, the scaling constant needs to satisfy $k_0 < \frac{1}{2} \sigma_{\tilde{\mathbf{X}}}$ where $\sigma_{\tilde{\mathbf{X}}}$ is largest eigenvalue of $\tilde{\mathbf{X}}^\top \tilde{\mathbf{X}}$ (see, e.g., She (2009); Bayram (2016)). Global and local convergence of the iterates can be proven for convex and non-convex penalties, respectively (Bauschke and Combettes, 2011; Bayram, 2016; She, 2009). In order to solve the primal update fast and robustly, we provide penalty-dependent initial parameter estimates $\tilde{\boldsymbol{\theta}}^{(i,0)}$. For the convex penalties II-III, we employ a “warm start” strategy and set $\tilde{\boldsymbol{\theta}}^{(i,0)} = \tilde{\boldsymbol{\theta}}^{(i-1)}$. When the non-convex penalty I is used, we set $\tilde{\boldsymbol{\theta}}^{(i,0)} = \tilde{\boldsymbol{\delta}}$, which is the solution of our robust initialization procedure, detailed in Section 3.2. This robust solution is also used to construct weights for penalty II. Following Zou (2006), we set $\mathbf{w} = |\tilde{\boldsymbol{\delta}}|^{-\nu}$ with $\nu = 1$. For penalties I and III, the weights are set to $\mathbf{w} = \mathbf{1}_{n+p}$.

The convergence of the dual descent approach naturally depends on the convergence of the algorithms solving the subproblems. We refer to Bertsekas (1982), Proposition 2.1 - 2.3, for convergence guarantees regarding the Lagrangian approach. With default parameters $\alpha = 0.95$ and $\nu = 1$, we see fast and robust performance of the algorithm under a wide range of simulation

and application scenarios. We summarize the estimation procedure in Algorithm 1.

Algorithm 1 Robust regression with compositional covariates

Given: \mathbf{X} , \mathbf{y} , $\lambda > 0$, $\nu = 1$, $\alpha = 0.95$.

Choose penalty function $P_\lambda(\cdot)$ and threshold operator $\Theta_\lambda(\cdot)$ from Table 1.

Set $i=0$, $\tilde{\boldsymbol{\theta}}^{(0)} = \ddot{\boldsymbol{\delta}}$ (initialization) and compute the scaling constant k_0 .

repeat

Define $\{\tilde{\mathbf{X}}, \tilde{\mathbf{y}}\}$ using (3.11), and set $j = 0$; $\tilde{\boldsymbol{\theta}}^{(i,0)} = \tilde{\boldsymbol{\theta}}^{(i)}$ (case II and III); $\tilde{\boldsymbol{\theta}}^{(i,0)} = \ddot{\boldsymbol{\delta}}$ (case I)

repeat

$$\tilde{\boldsymbol{\theta}}^{(i,j+1)} = \Theta_\lambda \left[\frac{\tilde{\mathbf{X}}^T \tilde{\mathbf{y}}}{k_0} + \left(\mathbf{I} - \frac{\tilde{\mathbf{X}}^T \tilde{\mathbf{X}}}{k_0} \right) \tilde{\boldsymbol{\theta}}^{(i,j)} \right]$$

$j \leftarrow j + 1$.

until convergence

return $\tilde{\boldsymbol{\theta}}^{(i+1)}$

$\boldsymbol{\eta}^{(i+1)} = \boldsymbol{\eta}^{(i)} + \mathbf{C}^T \boldsymbol{\theta}^{(i+1)}$ and then $i \leftarrow i + 1$.

until convergence

3.2 Robust initialization

Robust estimation procedures for linear models, including S-estimators (Rousseeuw and Yohai, 1984), MM-estimators (Yohai, 1987), the Θ -IPOD (She and Owen, 2011), and the Penalized Elastic-Net S-Estimator (PENSE) (Cohen Freue *and others*, 2017), are multi-stage estimators that comprise an initialization stage and one or several improvement stages. A common theme for the initialization stage is the use of resampling-based approaches in combination with robust loss functions (Maronna *and others*, 2006; Salibián-Barrera and Yohai, 2006). While most methods assume the model coefficients to be dense, a variant of the Θ -IPOD as well as the PENSE encourage sparse coefficients. However, the latter methods operate under the standard linear model and are not suited for the compositional setting. When solving the optimization problem

in (3.10) with penalty I or III, RobRegCC requires an initial estimate of the coefficients and the mean shift vector. Here, we apply the concept of principal sensitivity components (PSC) (Peña and Yohai, 1999) to the log-contrast model and propose the following resampling-based approach to robust initialization.

In the linear model, PSC analysis has been introduced for ordinary least squares (Peña and Yohai, 1999) and extended to robust ridge regression (Maronna, 2011) and robust sparse regression (Cohen Freue *and others*, 2017). PSC analysis relies on the idea of leave-one-out sensitivities of the following form. Given all samples, let \hat{y}_i be the estimated prediction of the model under consideration for observation i , and $\hat{y}_{i(j)}$ the corresponding prediction value with the j th observation removed. The sensitivity of the i th observation is then defined as

$$\mathbf{r}_i = [\hat{y}_i - \hat{y}_{i(1)}, \dots, \hat{y}_i - \hat{y}_{i(n)}]^\top, \quad i = 1, \dots, n. \quad (3.13)$$

The sensitivity matrix of all observation is defined as $\mathbf{R} = [\mathbf{r}_1, \dots, \mathbf{r}_n] \in \mathbb{R}^{n \times n}$. To identify potential outliers in the data, PSC analysis proceeds by first computing an eigenvalue decomposition of the matrix $\mathbf{R}\mathbf{R}^\top$. The eigenvectors \mathbf{u}_i of that matrix are called the principal sensitivity components (PSCs) of the matrix \mathbf{R} (Peña and Yohai, 1999). Observations that comprise extreme values with respect to the PSCs are deemed outliers and removed from the samples.

In RobRegCC, we adopt the protocol of PENSE (see (Cohen Freue *and others*, 2017) 2.2.) and propose a PSC-based analysis on the standard sparse log-contrast model (Shi *and others*, 2016), resulting in initial coefficient estimates on potentially outlier-free subsamples. We provide the exact computational protocol in Section 1.3 of the Supplementary Materials. The final outcome of the robust initialization procedure is the estimate $\ddot{\boldsymbol{\delta}} = [\ddot{\boldsymbol{\beta}}^\top \ddot{\boldsymbol{\gamma}}^\top]^\top$ which serves as initial starting point of the non-convex optimization procedure underlying RobRegCC with penalty P^H and forms the basis for weight construction in the adaptive Elastic Net penalty P^A , respectively.

3.3 Robust cross-validation model selection

An essential part of the RobRegCC workflow is data-driven tuning of the regularization parameter λ . Due to the lack of model selection criteria for the log-contrast model with corrupted observations, we introduce a novel robust cross-validation (R-CV) strategy.

We consider a λ -path with log-linearly spaced λ values in the interval $[\lambda_{\min}, \lambda_{\max}]$. We set the upper bound $\lambda_{\max} = \max(\|\mathbf{y} \mathbf{X}^T \mathbf{y}\|/\mathbf{w})$ and λ_{\min} to be the fraction of λ_{\max} at which the mean shift parameter $\hat{\gamma}$ comprises at most $n/2$ non-zeros (i.e., potential outliers). We split the model selection training data into $k = 10$ folds and perform cross-validation with a specifically tailored robust test statistics. For a given fold, we denote the n_{tr} training data by $\{\mathbf{y}_{tr}, \mathbf{X}_{tr}\}$, the n_{te} test data by $\{\mathbf{y}_{te}, \mathbf{X}_{te}\}$, and the parameters estimates on the training data at a given λ by $\{\hat{\boldsymbol{\theta}}_\lambda, \hat{\gamma}_\lambda\}$. As the standard mean-squared error is not an appropriate error measure in robust regression, we first compute the robust scale estimate $\hat{s}_{tr,\lambda}$ on the training data using

$$\hat{s}_{tr,\lambda} = \sqrt{\|\hat{\boldsymbol{\epsilon}}_{tr,\lambda}\|^2/n_{tr}} \quad \text{with} \quad \hat{\boldsymbol{\epsilon}}_{tr,\lambda} = \mathbf{y}_{tr} - \mathbf{X}_{tr}\hat{\boldsymbol{\theta}}_\lambda - \hat{\gamma}_\lambda.$$

The non-robust test sample residual is $\hat{\boldsymbol{\epsilon}}_{te,\lambda} = \mathbf{y}_{te} - \mathbf{X}_{te}\hat{\boldsymbol{\theta}}_\lambda$. To account for unknown outliers in a test sample, we calculate the scaled test error

$$\hat{\mathbf{r}}_{te,\lambda} = \hat{\boldsymbol{\epsilon}}_{te,\lambda}/\hat{s}_{tr,\lambda}$$

and then derive the robust scale estimate for the test sample using the median absolute deviation (MAD) (Rousseeuw and Hubert, 2011):

$$\hat{s}_{te,\lambda} = \text{MAD}(\hat{\mathbf{r}}_{te,\lambda}).$$

This scale estimate enables the removal of outliers in the test sample. Let $r_{te,j,\lambda}$ be the residual of the j th test sample. The set of outlier in the test sample O_{te} is

$$O_{te} = \{j \in \{1, \dots, n_{te}\} \mid |r_{te,j,\lambda}| > 2\hat{s}_{te,\lambda}\}.$$

After removing outliers O_{te} from the test sample, we denote the “clean” test data by $\{\mathbf{y}_{te}^c, \mathbf{X}_{te}^c\}$ and the “clean” residual by $\hat{\boldsymbol{\epsilon}}_{te,\lambda}^c = \mathbf{y}_{te}^c - \mathbf{X}_{te}^c \hat{\boldsymbol{\theta}}_\lambda$. We calculate the standard deviation $\hat{\sigma}_{te,\lambda}^c$ of the residual and introduce the following test statistics for robust cross-validation:

$$\hat{\epsilon}_{te,\lambda}^c = |\hat{\sigma}_{te,\lambda}^c - 1| \quad (3.14)$$

Let $\hat{\epsilon}_{te,i,\lambda}^c$ be the robust test statistics for fold i . We select the tuning parameter $\lambda_{\text{r-cv}}$ that minimizes the average k-fold robust cross-validation error $\bar{\epsilon}_{te,\lambda}^c = \frac{1}{k} \sum_{i=1}^k \hat{\epsilon}_{te,i,\lambda}^c$.

Figure 2 illustrates the typical behavior of R-CV model selection over the λ -path for simulated data (see Section 5 for details).

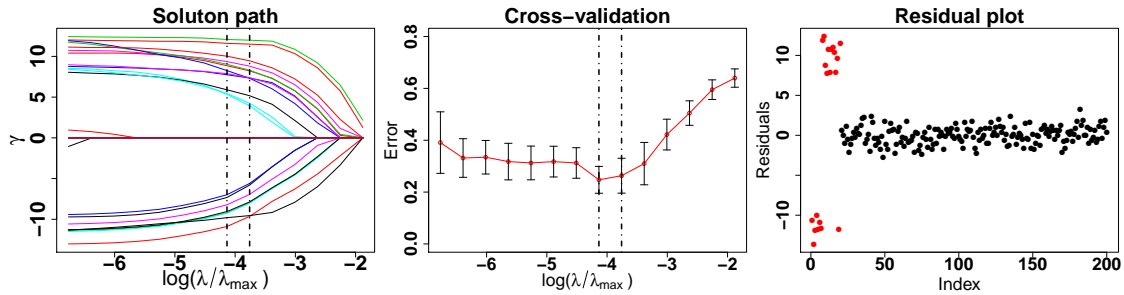


Figure 2. R-CV model selection: Left panel: Solution path of the mean shift parameter estimates $\hat{\gamma}$; middle panel: R-CV error $\bar{\epsilon}_{te,\lambda}^c$ (and standard error over k=10 folds) across the λ -path using RobRegCC with adaptive Elastic-net penalty. Vertical dashed line corresponds to the minimum R-CV error (left) and the one standard error (1SE) rule; right panel: Residuals $\hat{\epsilon}_{te,\lambda_{\text{r-cv}}}^c$ with outliers (red) identified using RobRegCC at minimum R-CV error.

REMARK 3.1 We highlight that the robust test statistics in (3.14) is also a useful measure for judging the performance of out-of-sample prediction, i.e., testing predictive power of an estimator on a hold-out (or validation) set after model selection. We will use this measure in simulation and real data analysis in Sections 5 and 6.

4. NON-ASYMPTOTIC ANALYSIS

We observe that the number of unknown parameters in the robust log-contrast regression model increases linearly with the sample size n . Hence, a finite sample analysis is desirable to understand the effect of the number of samples n , number of predictors p , and linear constraints k on the model prediction error. For simplicity, we perform the analysis of the robust model (2.7) with only compositional covariates \mathbf{Z} , i.e.,

$$\mathbf{y} = \mathbf{Z}\boldsymbol{\beta}^* + \boldsymbol{\gamma}^* + \boldsymbol{\epsilon}, \quad \text{s.t.} \quad \mathbf{C}^T \boldsymbol{\beta}^* = \mathbf{0}, \quad (4.15)$$

where $\boldsymbol{\beta}^* \in \mathbb{R}^p$ is the true coefficient, $\boldsymbol{\gamma}^* \in \mathbb{R}^n$ is the true mean shift, and $\boldsymbol{\epsilon}$ is the IID sub-Gaussian error with mean zero and variance σ^2 . $\mathbf{T}^* = \mathcal{J}(\boldsymbol{\gamma}^*)$ and $\mathbf{S}^* = \mathcal{J}(\boldsymbol{\beta}^*)$ denote the support index sets of $\boldsymbol{\gamma}^*$ and $\boldsymbol{\beta}^*$ such that $|\mathbf{T}^*| = t^*$ and $|\mathbf{S}^*| = s^*$, respectively.

From the general RobRegCC model formulation (2.8), the optimization problem for the reduced model (4.15) is given by

$$\{\widehat{\boldsymbol{\gamma}}_{\lambda_1}, \widehat{\boldsymbol{\beta}}_{\lambda_2}\} \equiv \arg \min_{\{\boldsymbol{\gamma}, \boldsymbol{\beta}\}} \left\{ \frac{1}{2} \|\mathbf{y} - \mathbf{Z}\boldsymbol{\beta} - \boldsymbol{\gamma}\|_2^2 + P_{\lambda_1}^1(\boldsymbol{\gamma}) + P_{\lambda_2}^2(\boldsymbol{\beta}) \right\} \quad \text{s.t.} \quad \mathbf{C}^T \boldsymbol{\beta} = \mathbf{0}. \quad (4.16)$$

In order to focus on the core issue, we consider dropping the quadratic component of the penalty functions (equivalent to setting $\alpha = 1$ as defined in Table 1) with separate tuning parameters $\{\lambda_1, \lambda_2\}$ for penalizing $\{\boldsymbol{\gamma}, \boldsymbol{\beta}\}$, respectively. Hereafter, for the ease of notation, we drop the subscript and denote the optimal solution of (4.16) by $\{\widehat{\boldsymbol{\beta}}, \widehat{\boldsymbol{\gamma}}\}$.

We define the model prediction error as $M(\widehat{\boldsymbol{\beta}} - \boldsymbol{\beta}^*, \widehat{\boldsymbol{\gamma}} - \boldsymbol{\gamma}^*)$ where $M(\mathbf{a}, \mathbf{b}) = \|\mathbf{Z}\mathbf{a} + \mathbf{b}\|_2^2$. Our analysis upper-bounds the prediction error in terms of the model bias and variance. For the unrestricted predictor matrix \mathbf{Z} , Theorem 4.1 provides a **slow rate bound** on the prediction error regardless of the type of sparsity-inducing penalty functions. Consequently, remark following the theorem states the oracle bound in case of ℓ^0 norm penalty (**case I**). Theorem 4.5 provides the result to attain the required oracle bound in case of ℓ^1 penalty under a compatibility condition on \mathbf{Z} , also referred as **fast rate bound**. Moreover, under some additional regularity assumptions,

the finite sample analysis of the prediction error can be extended i) to perform the asymptotic analysis; ii) to obtain the estimation error bound in various norms; and iii) to establish selection consistency of the parameter estimates (Lounici *and others*, 2011).

The proofs of our theorems rely on and extend prior work, in particular She (2016); She and Chen (2017); She (2017).

THEOREM 4.1 Consider the tuning parameter $\lambda_1 = A\lambda_a$ and $\lambda_2 = A\lambda_b$ with $\lambda_a = \sigma(\log(en))^{1/2}$, $\lambda_b = \sigma(\log(ep))^{1/2}$, and $A = \sqrt{ab}A_1$ for a sufficiently large A_1 satisfying $a \geq 2b > 0$. In terms of the optimal solution $\{\widehat{\boldsymbol{\beta}}, \widehat{\boldsymbol{\gamma}}\}$ of the optimization problem (4.16), we have

$$M(\widehat{\boldsymbol{\beta}} - \boldsymbol{\beta}^*, \widehat{\boldsymbol{\gamma}} - \boldsymbol{\gamma}^*) \lesssim M(\boldsymbol{\beta} - \boldsymbol{\beta}^*, \boldsymbol{\gamma} - \boldsymbol{\gamma}^*) + P_{\lambda_1}^1(\boldsymbol{\gamma}) + P_{\lambda_2}^2(\boldsymbol{\beta}) + (3 - k)\sigma^2,$$

for any $\{\boldsymbol{\beta}, \boldsymbol{\gamma}\}$. Here \lesssim means the inequality holds up to a multiplicative constant.

REMARK 4.2 Consider $P_{\lambda_1}^1(\boldsymbol{\gamma}) \lesssim \lambda_1^2$ and $P_{\lambda_2}^2(\boldsymbol{\beta}) \lesssim \lambda_2^2$. In case of $\boldsymbol{\beta} = \boldsymbol{\beta}^*$ and $\boldsymbol{\gamma} = \boldsymbol{\gamma}^*$, it follows from Theorem 4.1 that

$$M(\widehat{\boldsymbol{\beta}} - \boldsymbol{\beta}^*, \widehat{\boldsymbol{\gamma}} - \boldsymbol{\gamma}^*) \lesssim (3 - k)\sigma^2 + P_{\lambda_1}^1(\boldsymbol{\gamma}^*) + P_{\lambda_2}^2(\boldsymbol{\beta}^*) \lesssim (3 - k)\sigma^2 + \frac{\lambda_1^2}{2}t^* + \frac{\lambda_2^2}{2}s^*. \quad (4.17)$$

The oracle bound suggests that, with moderate number of outlier, the dependence of variance on t^* allows the parameter estimate to reduce model bias.

Corollary 4.3 Let us assume $0 \log 0 = 0$. Following the proofs of Theorem 4.1 and Lemma 1.1 in the SM, we have

$$M(\widehat{\boldsymbol{\beta}} - \boldsymbol{\beta}^*, \widehat{\boldsymbol{\gamma}} - \boldsymbol{\gamma}^*) \lesssim \inf_{(\boldsymbol{\beta}, \boldsymbol{\gamma}; t \leq \vartheta)} M(\boldsymbol{\beta} - \boldsymbol{\beta}^*, \boldsymbol{\gamma} - \boldsymbol{\gamma}^*) + \sigma^2 + P_{\lambda_2}^2(\boldsymbol{\beta}) + 2aL\sigma^2 \left(\vartheta + \vartheta \log \frac{en}{\vartheta} + 2 - k \right),$$

where t is cardinality of $\mathcal{J}(\boldsymbol{\gamma})$.

REMARK 4.4 Let us assume that \mathbf{y} is obtained after corrupting ϑ outcomes in the true generating model $\mathbf{y}^* = \mathbf{Z}\boldsymbol{\beta}^* + \boldsymbol{\epsilon}$. We define the breakdown point of the robust model as

$\epsilon^*(\widehat{\boldsymbol{\beta}}, \widehat{\boldsymbol{\gamma}}) = \min\{\vartheta/n; \sup_{|\mathcal{J}(\boldsymbol{\gamma}^*)| \leq \vartheta} \mathbb{E}[M(\widehat{\boldsymbol{\beta}} - \boldsymbol{\beta}^*, \widehat{\boldsymbol{\gamma}} - \boldsymbol{\gamma}^*)] = \infty\}$. From the Corollary 4.3, it follows that the finite sample breakdown point of the robust model is given by $\epsilon^* \geq (\vartheta + 1)/n$.

The parameter estimate obtained by solving the optimization problem (4.16) with ℓ^1 penalty attains the required oracle bound under the following compatibility conditions:

$$\mathbf{C1.} \quad (1 + \nu)|\boldsymbol{\gamma}'_{\mathbf{T}}|_1 \leq |\boldsymbol{\gamma}'_{\mathbf{T}^c}|_1 + \kappa_1 t^{1/2} \|\mathbf{P}_{\boldsymbol{\zeta}}^\perp \boldsymbol{\gamma}'\|_2$$

$$\mathbf{C2.} \quad (1 + \nu)|\boldsymbol{\beta}'_{\mathbf{S}}|_1 \leq |\boldsymbol{\beta}'_{\mathbf{S}^c}|_1 + \kappa_2 s^{1/2} \|\mathbf{P}_{\boldsymbol{\zeta}}(\boldsymbol{\zeta}\boldsymbol{\beta}'' + \boldsymbol{\gamma}')\|_2$$

for any suitable dimension $\boldsymbol{\gamma}'$, $\boldsymbol{\beta}'$, $\boldsymbol{\beta}''$, and the projection matrix $\mathbf{P}_{\boldsymbol{\zeta}}$ mapping the column space of $\boldsymbol{\zeta} \subseteq \mathbf{Z}$. Here, parameters κ_1 , κ_2 and ν are positive compatibility constants.

THEOREM 4.5 Consider the model matrix \mathbf{Z} in (4.15) satisfies the compatibility condition $\{\mathbf{C1}, \mathbf{C2}\}$, and the tuning parameter $\lambda_1 = A\lambda_a$ and $\lambda_2 = A\lambda_b$ with $\lambda_a = \sigma(\log(en))^{1/2}$, $\lambda_b = \sigma(\log(ep))^{1/2}$, and $A = \sqrt{ab}A_1$ for a sufficiently large A_1 satisfying $a \geq 2b > 0$. In terms of the optimal solution $\{\widehat{\boldsymbol{\beta}}, \widehat{\boldsymbol{\gamma}}\}$ of the optimization problem (4.16) with ℓ_1 penalty i.e., $P_{\lambda_1}^1(\boldsymbol{\gamma}) = \lambda_1|\boldsymbol{\gamma}|_1$ and $P_{\lambda_2}^2(\boldsymbol{\beta}) = \lambda_2|\boldsymbol{\beta}|_1$, we have

$$M(\widehat{\boldsymbol{\beta}} - \boldsymbol{\beta}^*, \widehat{\boldsymbol{\gamma}} - \boldsymbol{\gamma}^*) \lesssim M(\boldsymbol{\beta} - \boldsymbol{\beta}^*, \boldsymbol{\gamma} - \boldsymbol{\gamma}^*) + a\lambda_1^2(1 - \theta)^2\kappa_1^2t + a\lambda_2^2(1 - \theta)^2\kappa_2^2s + (3 - k)\sigma^2$$

where $\theta = \nu/(1 + \nu)$, $t = |\mathcal{J}(\boldsymbol{\gamma})|$ and $s = |\mathcal{J}(\boldsymbol{\beta})|$.

REMARK 4.6 Compared to the oracle bound in Equation (4.17), the variance term of the prediction error bound in Theorem 4.5 differs only by a constant multiplying factor.

5. SIMULATION BENCHMARKS

The overall purpose of the following simulation study is to evaluate RobRegCC's ability to simultaneously detect outliers and to perform sparse covariate selection when the underlying generative model is sparse. We follow the original simulation setup for the standard log-contrast model,

put forward in Shi *and others* (2016), and extend it by introducing different types of outliers in the response. We remark that the synthetic simulation setup does not reflect all aspects of high-throughput sequencing count data. Our simulations will be complemented by real gut microbiome data analysis in Section 6.

5.1 Benchmark setup

Following the simulation setup in Shi *and others* (2016), we generate count data $\mathbf{W} = [w_{ij}] \in \mathbb{R}^{n \times p}$ by simulating n instances of a multivariate random variable $\mathbf{w} \sim \text{Lognormal}(\boldsymbol{\mu}, \boldsymbol{\Sigma})$ with mean $\boldsymbol{\mu} = \{\log(p/2) \mathbf{1}_5, \mathbf{0}_{p-5}\} \in \mathbb{R}^p$ and covariance matrix $\boldsymbol{\Sigma} \in \mathbb{R}^{p \times p}$ such that $\Sigma_{ij} = 0.5^{|i-j|}$. We perform total-sum normalization of the count data \mathbf{W} and apply a log-transformation on the resulting compositions, thus arriving at covariates $\mathbf{Z} = [z_{ij}]_{n \times p}$ where $z_{ij} = \log \frac{w_{ij}}{\sum_{j=1}^p w_{ij}}$. For simplicity, we include a single non-compositional covariate in the form of an intercept $\mathbf{N} = \mathbf{1}_n$. Using the generative model in (2.5), we define $\mathbf{X} = [\mathbf{N} \mathbf{Z}]$ and set $\boldsymbol{\beta}^* = \{\beta_0, 1, -0.8, 0.4, 0, 0, -0.6, 0, 0, 0, 0, -1.5, 0, 1.2, 0, 0, 0.3, \mathbf{0}_{p-16}\}$ with $\beta_0 = 0.5$ (Shi *and others*, 2016). To model sub-compositional coherence, we consider the subcomposition constraint matrix \mathbf{C} with $k = 4$ subgroups of the form

$$\bar{\mathbf{C}}^T = \begin{bmatrix} \mathbf{1}_{p_1}^T & \mathbf{0} & \dots & \mathbf{0} \\ \mathbf{0} & \mathbf{1}_{p_2}^T & \dots & \mathbf{0} \\ \vdots & \vdots & \ddots & \vdots \\ \mathbf{0} & \mathbf{0} & \dots & \mathbf{1}_{p_4}^T \end{bmatrix}_{4 \times 23} \quad \text{and} \quad \mathbf{C}^T = [\mathbf{0}_{4 \times 1} \quad \bar{\mathbf{C}}^T \quad \mathbf{0}_{4 \times \{p-23\}}]_{4 \times (p+1)} \quad (5.18)$$

with $\mathbf{s} = [0, 10, 16, 20, 23]$, $p_i = \mathbf{s}_{i+1} - \mathbf{s}_i$, $i = 1, \dots, 4$, and index sets $\mathbb{A}_i = \{\mathbf{s}_i + 1, \dots, \mathbf{s}_{i+1}\}$.

We first generate the outlier-free response \mathbf{y} with error standard deviation $\sigma = \|\tilde{\mathbf{Z}}\boldsymbol{\beta}\|/(\sqrt{n} \times \text{SNR})$ where the signal-to-noise ratio (SNR) is set to $\text{SNR} = 3$. For fixed $n = 200$, we examine both the low- and high-dimensional scenario using $p = \{100, 300\}$.

To evaluate the ability of RobRegCC to detect outliers in the response, we considered the following scenarios for outlier generation. We used mean shift vectors $\boldsymbol{\gamma}$ with $\mathbf{O} = \{20\%, 15\%, 10\%, 5\%\}n$ outliers. Moderate outliers were generated by adding a shift of 6σ to the

true response \mathbf{y} , and large outliers by adding a shift of 8σ to the true response \mathbf{y} . We also considered the challenging setting where half of the \mathbf{O} outliers are leveraged. Leveraged instances in \mathbf{Z} (denoted by L in the simulation scenarios) were obtained by modifying the entries in the count data \mathbf{W} . The first $\mathbf{O}/2$ instances of \mathbf{W} are replaced by leveraged observations. A leveraged observation comprises a covariate (taxon) in each subgroup that is inflated to a large value while the remaining taxa in the subgroup are deflated to small values. For each subgroup of the k groups, we first identified the corresponding column subset matrix of \mathbf{W} , then arranged its first column in descending order after adding the constant 4, and then appended the remaining columns in ascending order. The first $\mathbf{O}/2$ instances of the rearranged matrix were the leveraged observations. We replicated each experimental setting $R = 100$ times.

For outlier identification, we measured performance in terms of the number of false positive (FP) (“swapping”) and false negative (FN) (“masking”) outliers. For the standard RobRegCC workflow, the number of FP and FN are derived by comparing the true set of outliers to the support set $\mathcal{J}(\hat{\gamma}_{\lambda_{r-cv}})$ after R-CV model selection. We denote these estimates by FP_1 and FN. We also provide a two-stage estimator, where we refit the standard log-contrast model on the identified inliers, compute the standard deviation of the residuals, and redefine all samples as inliers if their residuals are within the range of three standard deviations. The number of false positives for the two-stage estimator is denoted by FP_2 . Total mis-identification performance is measured using the Hamming distance, $HM = FN + FP_1$. We determine the quality of RobRegCC’s estimated sparse regression coefficients by refitting a standard log-contrast model on the support of $\mathcal{J}(\hat{\beta}_\lambda)$ at $\lambda = \lambda_{r-cv}$ using the inlier data only. The resulting refit $\hat{\beta}_{rf}$ estimates are compared to the oracle β^* via the scaled estimation error $Er(\beta) = 100\|\beta^* - \hat{\beta}_{rf}\|_2/p$.

5.2 *Simulation Results*

We summarize RobRegCC’s performance in the setting with large outliers (shift $s = 8\sigma$) in Table 2. Similar results for the moderate outlier (shift $s = 6\sigma$) scenario are available in Table S1 of the Supplementary Material. For comparison, we also consider the standard log-contrast model without mean shift (denoted by NR).

Table 2. Comparison of the non-robust [NR] model and the robust model, i.e., RobRegCC with the hard-ridge [H], the Elastic Net [E], and the adaptive Elastic Net [A] penalty function, in the simulation setting with high outliers ($n = 200$, $s = 8$) using the outlier identification measures false negative (FN) and false positive (FP), and the estimation error measure $\text{Er}(\beta)$. Here FP_1 and FP_2 refers to the pre and post false positive measures.

L	p	O	[A]				[H]				[E]				[NR]
			FN	γ		β	FN	γ		β	FN	γ		β	β
				FP_1	FP_2			Er	FP_1			FP_2	Er		
0	100	0	0.00	3.25	1.47	1.11	0.00	5.25	1.82	1.12	0.00	9.63	2.35	1.13	1.04
0	100	10	0.00	1.68	1.04	1.11	0.00	0.82	0.70	1.12	0.00	13.82	3.78	1.17	1.84
0	100	20	0.00	0.98	0.75	1.09	0.27	0.00	0.42	1.09	0.00	14.15	3.26	1.16	2.30
0	100	30	0.00	0.40	0.54	1.14	0.42	0.00	0.35	1.12	0.00	16.86	3.47	1.19	2.65
0	100	40	0.00	0.00	0.40	1.16	1.33	0.00	0.00	1.18	0.00	17.62	3.60	1.23	3.32
0	300	0	0.00	4.44	1.78	0.49	0.00	7.12	1.88	0.47	0.00	9.39	2.26	0.49	0.47
0	300	10	0.00	2.28	1.29	0.50	0.00	2.11	1.07	0.50	0.00	9.47	2.45	0.51	0.89
0	300	20	0.00	1.00	0.99	0.50	0.00	0.41	0.53	0.50	0.00	10.70	2.64	0.52	1.17
0	300	30	0.00	0.37	0.46	0.55	0.35	0.00	0.36	0.55	0.00	11.67	2.72	0.57	1.39
0	300	40	0.00	0.45	0.55	0.55	1.10	0.00	0.23	0.55	0.00	11.88	2.27	0.60	1.39
1	100	10	0.00	1.37	1.03	1.06	0.00	0.86	0.60	1.07	0.34	11.01	2.52	1.16	2.57
1	100	20	0.00	0.42	0.53	1.11	0.00	0.00	0.45	1.13	2.94	11.74	2.59	1.47	2.37
1	100	30	0.00	0.40	0.46	1.17	1.03	0.00	0.30	1.18	6.84	10.05	2.47	1.89	2.62
1	100	40	6.25	0.13	0.39	1.76	7.82	0.00	0.00	1.61	11.47	9.98	2.23	2.32	2.86
1	300	10	0.00	1.74	1.14	0.54	0.00	1.54	1.12	0.53	0.43	9.60	2.48	0.64	1.01
1	300	20	0.00	0.99	0.47	0.55	0.00	0.00	0.30	0.56	6.45	6.21	1.55	1.14	1.15
1	300	30	0.00	0.84	0.60	0.55	0.41	0.00	0.36	0.52	11.26	6.20	1.76	1.16	1.12
1	300	40	1.44	0.38	0.35	0.68	0.99	0.00	0.28	0.61	16.64	7.93	1.63	1.03	1.05

We observed that RobRegCC with hard-ridge(H) and adaptive penalty(A) consistently outperformed the other methods both in terms of outliers identification and regression coefficient estimation. This highlights the importance of our novel PSC-based initialization routine on subsequent estimation. RobRegCC with the Elastic Net penalty (E) performs well in the absence of leveraged ($L = 0$) outliers but drastically deteriorates when the outliers are leveraged ($L = 1$). All

estimators were more prone to swapping (higher FP values) than masking effects. This was also reflected in the slightly reduced performance of RobRegCC compared to the standard log-contrast model in the absence of outliers ($O = 0$). Here, the NR approach achieved the best performance in scaled estimation error for the regression coefficients ($Er = 1.04$ for NR compared to $Er = 1.11$, $Er = 1.12$, and $Er = 1.13$, for penalties P^A , P^H , and P^E , respectively). This is due the fact that the standard log-contrast model could take all sample into account whereas the other estimators suffered from small swapping effects.

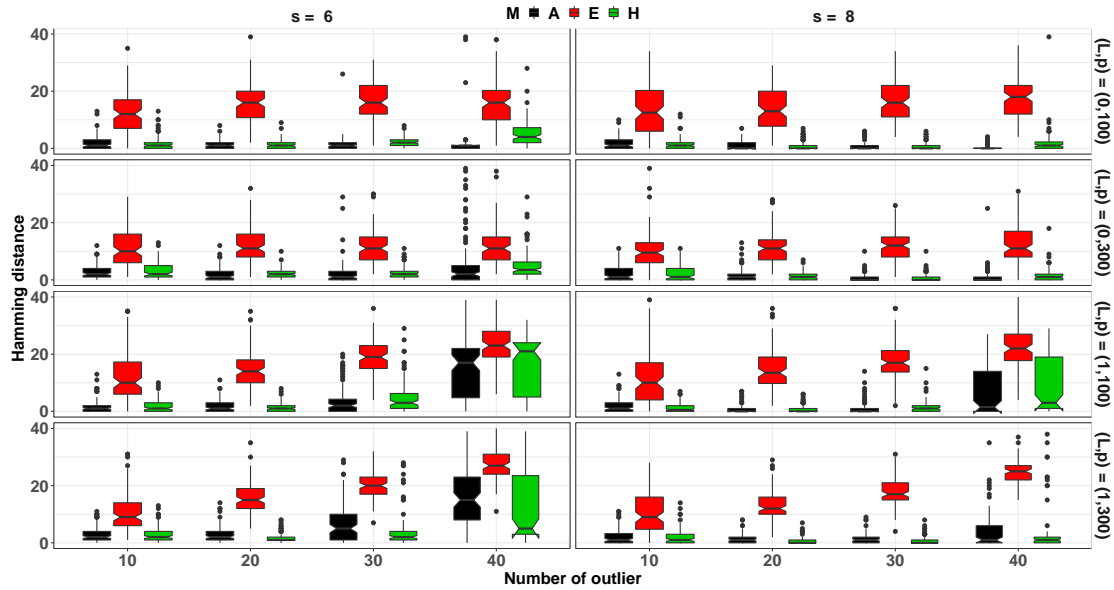


Figure 3. RobRegCC's outlier detection performance in terms of Hamming distance (HM) on simulated data ($p = \{100, 300\}$, $n = 200$) with outlier observations shifted by $s = 6\sigma$ (left column) and $s = 8\sigma$ (right column) and number of outliers $O = \{10, 20, 30, 40\}$. $L = \{0, 1\}$ indicates the absence or presence of leveraged outliers.

While the overall performance of the data-driven R-CV model selection scheme was encouraging, we consistently observed slight over-selection of potential outliers in RobRegCC ($F_N \approx 0$ for most settings), in particular with the P^E penalty. This behavior was alleviated by the heuristic two-stage estimator whose number of false positives FP_2 was consistently lower than FP_1 for RobRegCC with P^E . The two-stage estimator thus offers a computationally efficient robust

estimation alternative when no leveraged outliers are present.

Figure 3 summarizes RobRegCC’s overall outlier detection performance across all simulation scenarios using the Hamming distance. We again observed excellent performance of RobRegCC with hard-ridge(H) and adaptive penalty(A). The performance decreased only in the setting with a high number of leveraged outliers ($> 15\%$). The performance of RobRegCC with Elastic Net penalty (E) showed the expected sub-optimal performance across all scenarios.

6. ROBUST REGRESSION ON GUT MICROBIOME DATA

We next applied the RobRegCC workflow to learn robust and predictive models of soluble CD14 (sCD14) measurements, an immune marker related to chronic inflammation and monocyte activation, from gut microbiome samples of HIV patients. The data set comprises $n = 151$ observations of sCD14 measurements and aggregated 16S rRNA amplicon data across $p = 60$ bacterial genera. In Rivera-Pinto *and others* (2018), the data set has been used to highlight the performance of the balance selection scheme (`selbal`), a greedy step-wise log-contrast modeling method. We provide three comparative analyses on this dataset, showcasing the flexibility of RobRegCC.

6.1 Comparison of RobRegCC with standard log-contrast approaches

We modeled the sCD14 measurements as continuous response $\mathbf{y} \in \mathbb{R}^n$, considered the clr transform of the relative genera abundances as compositional covariates $\mathbf{Z} \in \mathbb{R}^{n \times p}$, and used an intercept $\mathbf{N} = \mathbf{1}_n$ as non-compositional covariate.

To facilitate comparison with `selbal`, we first considered RobRegCC with the standard zero-sum constraint $\mathbf{C} = \mathbf{1}_p^T$, analyzed model performance in terms of overall R^2 , and compared the set of sparse predictors. For `selbal`, Rivera-Pinto *and others* (2018) report a log-contrast model with four genera: [g]Subdoligranulum and [f]Lachnospiraceae-[g].Incertae.Sedis (in the numerator) and [f]Lachnospiraceae-[g].unclassified and [g]Collinsella (in the denominator). The

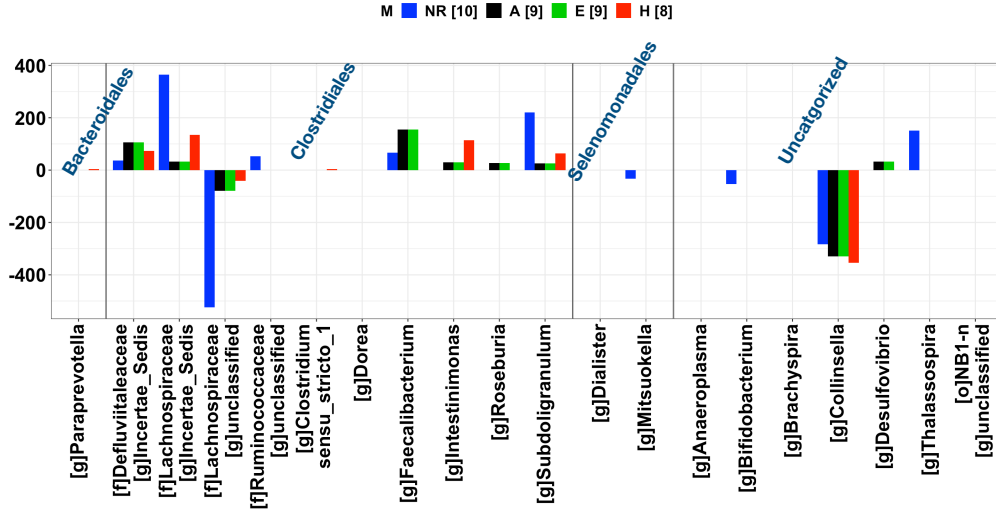


Figure 4. RobRegCC log-contrast predictors for sCD14 HIV dataset with zero-sum constraint $\mathbf{C} = \mathbf{1}_p$, the three penalty functions (H,E,A), and without mean shift (denoted “non-robust” (NR)) (number of non-zero coefficients of the different models are shown in parenthesis). Predictor labels correspond to genera names at the finest taxonomic resolution available (class(c), family(f), genus(g) and order(o)).

`selbal` log-contrast model fit on all data achieves an $R^2 = 0.281$. RobRegCC identified nine outliers with the P^A and P^E penalties, and five outliers with the P^H penalty, respectively (see Figures S1 –S3 in the Supplementary material). *RobRegCC* infers slightly less sparse models with eight to ten predictors. After removal of the outliers, *RobRegCC*’s models achieved considerable higher R^2 ’s, ranging from 0.53 (E), to 0.57 (H), and 0.63 (A), respectively. Figure 4 reports the identified set of genera in the respective models.

Consistent with the `selbal` findings, the robust models included the four genera `[g]Subdoligranulum`, `[f]Lachnospiraceae-[g]Incertae-Sedis`, `[f]Lachnospiraceae-[g]-unclassified`, and `[g]Collinsella`. In addition, all RobRegCC models also identified the genera `[f]Defluviitaleacea-[g]IncertaeSedis` and `[g]Intestinimonas` to be positively associated with sCD14. The RobRegCC models with the (adaptive) Elastic Net penalties identified the genus `[g]Faecalibacterium` to be positively associated with sCD14 as well. The standard non-robust [NR] log-contrast model identified several genera, not present in the robust models, including

[g]Bifidobacterium, [g]Mitsukella, and [g]Thalassospira.

To give a fair evaluation of the out-of-sample predictive performance of the RobRegCC models, we randomly split the data 100 times into two sets with 90% ($n_{\text{tro}} = 136$) samples $\{\mathbf{y}_{\text{tro}}, \mathbf{X}_{\text{tro}}\}$ for training and 10% ($n_{\text{teo}} = 15$) samples $\{\mathbf{y}_{\text{teo}}, \mathbf{X}_{\text{teo}}\}$ for out-of-sample prediction. We used the robust test statistic, introduced in (3.14), to measure robust out-of-sample prediction error. Table 3 reports the mean and standard deviation (in parenthesis) of the the robust error $\epsilon_{\text{teo}, \lambda_{\text{cv}}}$, average sample size $n_{\text{teo}, r}$ after outlier removal in the test data, and the percentage of outliers $O_{\text{tro}}\%$ identified in the training phase for both robust and non-robust models. The comparison also includes the `selbal` model with the four genera (Rivera-Pinto *and others*, 2018) as predictors, denoted by NR_0 . We observed that the robust approaches showed superior estimation performance (i.e., lower test error) and identified roughly 5-6% of the samples as outliers.

Table 3. Predictive modeling of sCD14 data with $\mathbf{C} = \mathbf{1}_p$: Mean and standard deviation (in parenthesis) of the out-of-sample scaled test error $\epsilon_{\text{teo}, \lambda_{\text{cv}}}$, the “clean” sample size ($n_{\text{teo}, r}$) on the test data, and the percentage of outliers $O_{\text{tro}}\%$ identified in the training data.

	A	E	H	NR	NR ₀
$\epsilon_{\text{teo}, \lambda_{\text{cv}}}$	0.28 (0.20)	0.29 (0.22)	0.29 (0.20)	0.36 (0.20)	0.34 (0.18)
$n_{\text{teo}, r}$	13.18 (1.52)	13.68 (0.98)	13.22 (1.46)	13.41 (1.13)	13.64 (1.01)
$O_{\text{tro}}\%$	4.84 (1.76)	6.09 (2.05)	4.78 (1.39)	0.00 (0.00)	0.00 (0.00)

6.2 Robust regression with subcompositional coherence

The process of measuring relative microbial species abundances introduces biases at multiple experimental stages (Pollock *and others*, 2018), including taxonomy-dependent biases due to some microbes being more resistant to cell lysis or variable specificities of the primer sets. Such taxonomic biases can be mitigated by enforcing sub-compositional coherence with respect to taxonomic grouping (Shi *and others*, 2016). Here, we extended the analysis from before with the subcompositional coherence imposed at the order level, resulting in a constraint matrix \mathbf{C} (see Equation 1.19 in the Supplementary Material) with $k = 6$ subcompositions. The taxa with known

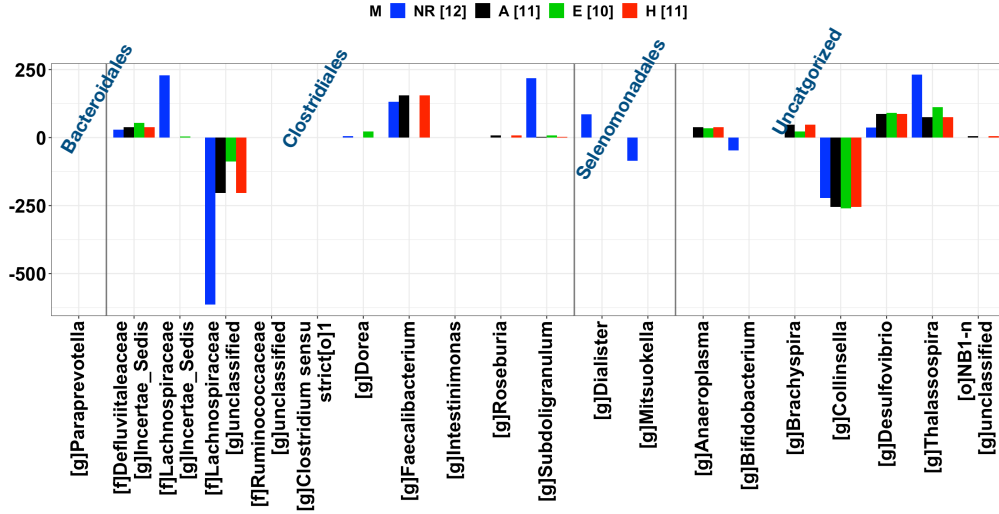


Figure 5. RobRegCC log-contrast predictors on the sCD14 HIV dataset with subcompositional constraints on order level, the three penalty functions (H,E,A), and without mean shift (denoted “non-robust” (NR)) (number of non-zero coefficients of the different models are shown in parenthesis). Predictor labels correspond to genera names at the finest taxonomic resolution available (class(c), family(f), genus(g) and order(o)).

order information were grouped into five subcompositions. Uncategorized taxa formed the sixth subcomposition.

RobRegCC identified nine outliers with the P^A and the P^H penalties and ten outliers with P^E , respectively. The subcompositional constraint induced slightly denser models with ten to twelve predictors while simultaneously maintaining superior out-of-sample prediction performance (see Table 4) and model R^2 's (see Figure S9 –S12 in the Supplementary Material), when compared to the `selbal` or the non-robust model.

Table 4. Predictive modeling of sCD14 data with subcompositional constraint: Mean and standard deviation (in parenthesis) of the out-of-sample scaled test error $\epsilon_{teo,\lambda_{cv}}$, the “clean” sample size ($n_{teo,r}$) on the test data, and the percentage of outliers $O_{tro}\%$ identified in the training data.

	A	E	H	NR	NR ₀
$\epsilon_{teo,\lambda_{cv}}$	0.29 (0.19)	0.26 (0.19)	0.29 (0.20)	0.34 (0.18)	0.34 (0.19)
$n_{teo,r}$	13.66 (0.99)	13.61 (0.96)	13.61 (0.99)	13.66 (1.04)	13.71 (0.96)
$O_{tro}\%$	4.88 (1.58)	6.28 (1.91)	4.78 (1.75)	0.00 (0.00)	0.00 (0.00)

Figure 5 reports the selected microbial species that were associated with the

sCD14 inflammation marker. With the subcompositional coherence at order level, [f]Defluviitaleacea_[g]IncertaeSedis, [f]Lachnospiraceae_[g]IncertaeSedis, and [g]Faecalibacterium were associated with sCD14. The models also include the genera [g]Desilfovibrio and [g]Thalassospira and discard the genus [f]Lachnospiraceae_[g]IncertaeSedis, when compared to the previous analysis. The robust models only selected predictors in the Clostridiales and the Uncategorized subcomposition.

6.3 Robustness to data mislabeling

A common source of error in analyzing microbial datasets, in particular those coming from public resources such as NCBI’s SRA (<https://www.ncbi.nlm.nih.gov/sra>), stems from insufficient documentation of the correspondence between data files comprising raw read data and their associated experimental meta-information. Missing or mislabeled meta-information is not uncommon and hinders large-scale meta- or re-analysis of many public data. To show that RobRegCC can deal with potential data mislabeling, we emulated such a scenario on the sCD14 dataset by generating $O = 10$ mislabeled observations. We actively interchanged the $O/2$ largest and $O/2$ smallest entries in the response \mathbf{y} while keeping the corresponding rows in \mathbf{Z} unchanged (see Figure 6(a)). We observed that non-robust regression on the mislabeled data resulted in a significant drop in model fit ($R^2 = 0.065$, see Figure S8 in the Supplementary Material). RobRegCC’s performance was not affected by the corrupted observations ($R^2 = 0.69$ (H), 0.55 (E), and 0.55 (A), see Figure S8 in the Supplementary Material). We further compared the similarity between RobRegCC’s predictors on the original data $\hat{\beta}_o$ and the predictors $\hat{\beta}_m$ on the mislabeled data by measuring the relative error $\text{err}_{rel} = 100\|\hat{\beta}_o - \hat{\beta}_m\|/\|\hat{\beta}_o\|$ and the support mismatch via the Hamming distance $\text{HM}(\hat{\beta}_m)$. Figures 6(b),(c) summarize the error estimates. The RobRegCC model with adaptive Elastic Net penalty outperformed all other methods in both error measures, shared five predictors with the regression model on the original data, and correctly identified seven mislabeled data

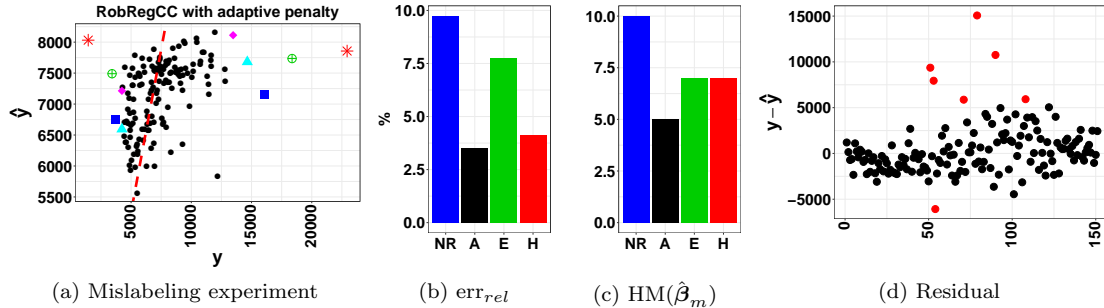


Figure 6. Comparison of the robust and non-robust approaches on mislabeled data: (a) Color coded observations of the sCD14 measurements (y) on the two side of the red dotted line are actively interchanged; (b) relative error $err_{rel} = 100\|\hat{\beta}_o - \hat{\beta}_m\|/\|\hat{\beta}_o\|$ (see main text for explanation);(c) support mismatch $HM(\hat{\beta}_m)$ (see main text for explanation);(d) estimated residual plot with outliers identified in red dots using RobRegCC with adaptive Elastic Net penalty.

points as outliers (Figure 6(d)).

7. DISCUSSION AND CONCLUSION

In this contribution, we have presented RobRegCC, a robust log-contrast regression framework that allows simultaneous outlier and sparse model coefficient identification for regression problems with compositional and non-compositional covariates. The approach combines the idea of mean shift estimation in linear regression with robust initialization and penalization for linear log-contrast regression (Aitchison and Bacon-Shone, 1984). We have tackled the resulting over-specified model parameter estimation problem via regularization with suitable sparsity-inducing penalty functions, including the hard-ridge, the Elastic Net, and a novel adaptive Elastic Net penalty. While the estimation approach with the Elastic Net penalty lacks the ability to handle masking and swapping effect (She and Owen, 2011), the adaptive Elastic Net and the hard-ridge penalties alleviate this problem but require initial robust estimates of the parameters to construct appropriate Elastic Nets weights or good initial parameter estimates, respectively. For the robust initialization step, we have used the concept of principal sensitivity component analysis (Peña and Yohai, 1999). RobRegCC also includes (i) a general Lagrangian-based optimization procedure

to solve the underlying optimization problem with any of the available penalty functions and (ii) a novel robust prediction error measure and cross-validation scheme that may be of independent interest. We have shown, on simulated and real compositional microbiome data, the validity and generality of our approach and have developed novel theoretical results that give prediction error bounds for the RobRegCC estimators in the finite sample setting. In practice, we recommend using RobRegCC with the adaptive Elastic Net penalty, since this estimator showed superior prediction and consistency performance on the majority of the experimental scenarios.

Future computational efforts will include exploring and implementing other computationally efficient optimization strategies, including recent path-based algorithms for log-contrast regression (Gaines *and others*, 2018). On the theoretical side, we will analyze the variable selection properties of the RobRegCC model estimators. A natural extension of our modeling framework is robust logistic regression when responses are given as class indicators rather than continuous variables. In summary, we believe that our RobRegCC framework provides a useful tool for statisticians and computational biologists that want to robustly solve regression problems with compositional covariates.

REFERENCES

- AITCHISON, JOHN. (1982). The statistical analysis of compositional data. *Journal of the Royal Statistical Society. Series B (Methodological)*, 139–177.
- AITCHISON, J. (2003). A concise guide to compositional data analysis. *2nd Compositional Data Analysis Workshop; Girona, Italy*.
- AITCHISON, JOHN AND BACON-SHONE, JOHN. (1984). Log contrast models for experiments with mixtures. *Biometrika* **71**(2), 323–330.
- ANTONIADIS, ANESTIS. (2007). Wavelet methods in statistics: some recent developments and

- their applications. *Statistics Surveys* **1**(0), 16–55.
- ANTONIADIS, ANESTIS AND FAN, JIANQING. (2001). Regularization of Wavelet Approximations. *Journal of the American Statistical Association* **96**, 939–967.
- BATES, STEPHEN AND TIBSHIRANI, ROBERT. (2018). Log-ratio lasso: Scalable, sparse estimation for log-ratio models. *Biometrics* **0**(0).
- BAUSCHKE, HEINZ H AND COMBETTES, PATRICK L. (2011). Convex Analysis and Monotone Operator Theory in Hilbert Spaces. *Book*, 1—469.
- BAYRAM, ILKER. (2016). On the Convergence of the Iterative Shrinkage/Thresholding Algorithm With a Weakly Convex Penalty. *IEEE Transactions on Signal Processing* **64**(6), 1597–1608.
- BERTSEKAS, DIMITRI P DP. (1982). *Constrained optimization and Lagrange multiplier methods*.
- BRICEÑO-ARIAS, LUIS AND RIVERA, SERGIO LÓPEZ. (2018). A projected primal-dual splitting for solving constrained monotone inclusions.
- CALLAHAN, BENJAMIN J., MCMURDIE, PAUL J. AND HOLMES, SUSAN P. (2017). Exact sequence variants should replace operational taxonomic units in marker-gene data analysis. *ISME Journal* **11**(12), 2639–2643.
- COHEN FREUE, GABRIELA V, KEPPLINGER, DAVID, SALIBIÁN-BARRERA, MATÍAS AND SMUCLER, EZEQUIEL. (2017). PENSE: A Penalized Elastic Net S-Estimator.
- COMBETTES, PATRICK L. AND MÜLLER, CHRISTIAN L. (2020). Regression Models for Compositional Data: General Log-Contrast Formulations, Proximal Optimization, and Microbiome Data Applications. *Statistics in Biosciences* (0123456789).
- COMBETTES, PATRICK L. AND PESQUET, JEAN CHRISTOPHE. (2011). Proximal splitting methods in signal processing. *Springer Optimization and Its Applications* **49**, 185–212.

- COMBETTES, PATRICK L. AND PESQUET, JEAN CHRISTOPHE. (2012). Primal-Dual Splitting Algorithm for Solving Inclusions with Mixtures of Composite, Lipschitzian, and Parallel-Sum Type Monotone Operators. *Set-Valued and Variational Analysis* **20**(2), 307–330.
- DAUBECHIES, INGRID, DEFRISE, MICHEL AND DE MOL, CHRISTINE. (2004). An iterative thresholding algorithm for linear inverse problems with a sparsity constraint. *Communications on Pure and Applied Mathematics*.
- EDGAR, ROBERT C. (2016). UNOISE2: improved error-correction for Illumina 16S and ITS amplicon sequencing. *bioRxiv* <https://www.biorxiv.org/content/early/2016/10/15/081257>.
- FRIEDMAN, JONATHAN AND ALM, ERIC J. (2012). Inferring correlation networks from genomic survey data. *PLoS computational biology* **8**(9), e1002687.
- GAINES, BRIAN R., KIM, JUHYUN AND ZHOU, HUA. (2018). Algorithms for Fitting the Constrained Lasso. *Journal of Computational and Graphical Statistics* **27**(4), 861–871.
- GANNAZ, IRÈNE. (2007). Robust estimation and wavelet thresholding in partially linear models. *Statistics and Computing* **17**(4), 293–310.
- HOLMES, IAN, HARRIS, KEITH AND QUINCE, CHRISTOPHER. (2012). Dirichlet multinomial mixtures: Generative models for microbial metagenomics. *PLoS ONE* **7**(2).
- HRON, K, FILZMOSER, P AND THOMPSON, K. (2012). Linear regression with compositional explanatory variables. *Journal of Applied Statistics* **39**(5), 1115–1128.
- HUTTENHOWER, CURTIS, GEVERS, DIRK, KNIGHT, ROB, ABUBUCKER, SAHAR, BADGER, JONATHAN H., CHINWALLA, ASIF T., CREASY, HEATHER H., EARL, ASHLEE M., FITZGERALD, MICHAEL G., FULTON, ROBERT S., GIGLIO, MICHELLE G., HALLSWORTH-PEPIN, KYMBERLIE, LOBOS, ELIZABETH A., MADUPU, RAMANA, MAGRINI, VINCENT, MARTIN, JOHN C., MITREVA, MAKEDONKA, MUZNY, DONNA M., SODERGREN, ERICA J. *and others*.

- (2012). Structure, function and diversity of the healthy human microbiome. *Nature* **486**(7402), 207–214.
- LEE, YOONKYUNG, MACEACHERN, STEVEN N. AND JUNG, YOONSUH. (2012). Regularization of Case-Specific Parameters for Robustness and Efficiency. *Statistical Science* **27**(3), 350–372.
- LIN, WEI, SHI, PIXU, FENG, RUI AND LI, HONGZHE. (2014). Variable selection in regression with compositional covariates. *Biometrika* **101**(4), 785–797.
- LOUNICI, KARIM, PONTIL, MASSIMILIANO, VAN DE GEER, SARA, TSYBAKOV, ALEXANDRE B AND OTHERS. (2011). Oracle inequalities and optimal inference under group sparsity. *The Annals of Statistics* **39**(4), 2164–2204.
- MARONNA, R.A., MARTIN, R.D. AND YOHAI, V.J. (2006). *Robust statistics*.
- MARONNA, RICARDO A. (2011). Robust ridge regression for high-dimensional data. *Technometrics* **53**.
- MCDONALD, DANIEL, HYDE, EMBRIETTE, DEBELIUS, JUSTINE W., MORTON, JAMES T., GONZALEZ, ANTONIO, ACKERMANN, GAIL, AKSENOV, ALEXANDER A., BEHSAZ, BAHAR, BRENNAN, CAITRIONA, CHEN, YINGFENG, DERIGHT GOLDASICH, LINDSAY, DORRESTEIN, PIETER C., DUNN, ROBERT R., FAHIMIPOUR, ASHKAAN K., GAFFNEY, JAMES, GILBERT, JACK A., GOGUL, GRANT, GREEN, JESSICA L., HUGENHOLTZ, PHILIP, HUMPHREY, GREG, HUTTENHOWER, CURTIS, JACKSON, MATTHEW A., JANSSEN, STEFAN, JESTE, DILIP V., JIANG, LINGJING, KELLEY, SCOTT T., KNIGHTS, DAN, KOSCIOLEK, TOMASZ, LADAU, JOSHUA, LEACH, JEFF, MAROTZ, CLARISSE, MELESHKO, DMITRY, MELNIK, ALEXEY V., METCALF, JESSICA L., MOHIMANI, HOSEIN, MONTASSIER, EMMANUEL, NAVAS-MOLINA, JOSE, NGUYEN, TANYA T., PEDDADA, SHYAMAL, PEVZNER, PAVEL, POLLARD, KATHERINE S., RAHNAVARD, GHOLAMALI, ROBBINS-PIANKA, ADAM, SANGWAN, NASEER,

- SHORENSTEIN, JOSHUA, SMARR, LARRY, SONG, SE JIN, SPECTOR, TIMOTHY, SWAFFORD, AUSTIN D., THACKRAY, VARYKINA G., THOMPSON, LUKE R., TRIPATHI, ANUPRIYA, VÁZQUEZ-BAEZA, YOSHIKI, VRBANAC, ALISON, WISCHMEYER, PAUL, WOLFE, ELAINE, ZHU, QIYUN, *and others.* (2018). American gut: an open platform for citizen science microbiome research. *mSystems* **3**(3).
- NASRABADI, NASSER M, TRAN, TRAC D AND NGUYEN, NAM. (2011). Robust Lasso with missing and grossly corrupted observations. In: *Advances in Neural Information Processing Systems*. pp. 1881—1889.
- PEÑA, DANIEL AND YOHAI, VICTOR. (1999). A Fast Procedure for Outlier Diagnostics in Large Regression Problems. *Journal of the American Statistical Association* **94**(446), 434–445.
- POLLOCK, JOLINDA, GLENDINNING, LAURA, WISEDCHANWET, TRONG AND WATSON, MICK. (2018). The madness of microbiome: attempting to find consensus best practice for 16s microbiome studies. *Appl. Environ. Microbiol.* **84**(7), e02627–17.
- RANDOLPH, TIMOTHY W., ZHAO, SEN, COPELAND, WADE, HULLAR, MEREDITH AND SHOJAIE, ALI. (2018). Kernel-penalized regression for analysis of microbiome data. *Annals of Applied Statistics* **12**(1), 540–566.
- RIVERA-PINTO, J, EGOZCUE, JJ, PAWLOWSKY-GLAHN, VERA, PAREDES, RAUL, NOGUERA-JULIAN, MARC AND CALLE, ML. (2018). Balances: a new perspective for microbiome analysis. *MSystems* **3**(4).
- ROUSSEEUW, PETER AND YOHAI, VICTOR. (1984). Robust Regression by Means of S-Estimators. In: Franke, Jürgen, Härdle, Wolfgang and Martin, Douglas (editors), *Robust and Nonlinear Time Series Analysis*, Volume 26, Lecture Notes in Statistics. Springer US, pp. 256–272.

- ROUSSEEUW, PETER J AND HUBERT, MIA. (2011). Robust statistics for outlier detection. *Wiley Interdisciplinary Reviews: Data Mining and Knowledge Discovery* **1**(1), 73–79.
- SALIBIAN-BARRERA, MATIAS AND YOHAI, VICTOR J. (2006). A fast algorithm for S-regression estimates. *Journal of Computational and Graphical Statistics* **15**(2), 414–427.
- SHE, YIYUAN. (2009). Thresholding-based iterative selection procedures for model selection and shrinkage. *Electron. J. Statist.* **3**, 384–415.
- SHE, YIYUAN. (2012). An iterative algorithm for fitting nonconvex penalized generalized linear models with grouped predictors. *Computational Statistics & Data Analysis* **56**(10), 2976–2990.
- SHE, YIYUAN. (2016). On the Finite-Sample Analysis of Θ -estimators. *Electronic Journal of Statistics*.
- SHE, YIYUAN. (2017). Selective factor extraction in high dimensions. *Biometrika* **104**(1), 97–110.
- SHE, Y. AND CHEN, K. (2017). Robust reduced-rank regression. *Biometrika*.
- SHE, YIYUAN AND OWEN, ART B. (2011). Outlier detection using nonconvex penalized regression. *Journal of the American Statistical Association* **106**(494), 626–639.
- SHI, PIXU, ZHANG, ANRU, LI, HONGZHE AND OTHERS. (2016). Regression analysis for microbiome compositional data. *The Annals of Applied Statistics* **10**(2), 1019–1040.
- SUN, ZHE, XU, WANLI, CONG, XIAOMEI AND CHEN, KUN. (2018). Log-Contrast Regression with Functional Compositional Predictors: Linking Preterm Infant’s Gut Microbiome Trajectories in Early Postnatal Period to Neurobehavioral Outcome. pp. 1–38.
- SUNAGAWA, SHINICHI, COELHO, LUIS PEDRO, CHAFFRON, SAMUEL, KULTIMA, JENS ROAT, LABADIE, KARINE, SALAZAR, GUILLEM, DJAHANSCHIRI, BARDYA, ZELLER, GEORG, MENDE, DANIEL R., ALBERTI, ADRIANA, CORNEJO-CASTILLO, FRANCISCO M., COSTEA, PAUL I.,

- CRUAUD, CORINNE, D’OVIDIO, FRANCESCO, ENGELEN, STEFAN, FERRERA, ISABEL, GASOL, JOSEP M., GUIDI, LIONEL, HILDEBRAND, FALK, KOKOSZKA, FLORIAN, LEPOIVRE, CYRILLE, LIMA-MENDEZ, GIPSI, POULAIN, JULIE, POULOS, BONNIE T., ROYO-LLONCH, MARTA, SARMENTO, HUGO, VIEIRA-SILVA, SARA, DIMIER, CÉLINE, PICHERAL, MARC, SEARSON, SARAH, KANDELS-LEWIS, STEFANIE, , BOWLER, CHRIS, DE VARGAS, COLOMBAN, GORSKY, GABRIEL, GRIMSLEY, NIGEL, HINGAMP, PASCAL, IUDICONE, DANIELE, JAILLON, OLIVIER, NOT, FABRICE, OGATA, HIROYUKI, PESANT, STEPHANE, SPEICH, SABRINA, STEMMANN, LARS, SULLIVAN, MATTHEW B., WEISSENBACH, JEAN, WINCKER, PATRICK, KARSENTI, ERIC, RAES, JEROEN, ACINAS, SILVIA G. *and others.* (2015). Structure and function of the global ocean microbiome. *Science* **348**(6237).
- THOMPSON, LUKE R., SANDERS, JON G., McDONALD, DANIEL, . . . , ZHANG, QIKUN AND ZHAO, HONGXIA. (2017). A communal catalogue reveals Earth’s multiscale microbial diversity. *Nature* **551**(7681), 457–463.
- WANG, TAO AND ZHAO, HONGYU. (2017). Structured subcomposition selection in regression and its application to microbiome data analysis. *Annals of Applied Statistics* **11**(2), 771–791.
- YOHAI, V J. (1987). High Breakdown Point and High Efficiency Robust Estimates for Regression. *Annals of Statistics* **15**.
- ZOU, HUI. (2006). The Adaptive Lasso and Its Oracle Properties. *Journal of the American Statistical Association* **101**, 1418–1429.
- ZOU, HUI AND HASTIE, TREVOR J. (2005). Regularization and variable selection via the elastic net. *Journal of the Royal Statistical Society: Series B* **67**(2), 301–320.

8. SUPPLEMENTARY MATERIAL

SUPPLEMENTARY MATERIAL

1.1 *Simulation: Model performance in the simulation setting with moderate outliers*

Table S1. Comparison of the non-robust [NR] model and the robust model, i.e., RobRegCC with the hard-ridge [H], the Elastic Net [E], and the adaptive Elastic Net [A] penalty function, in the simulation setting with moderate outliers ($n = 200$, $s = 6$) using the outlier identification measures false negative (FN) and false positive (FP), and the estimation error measure $\text{Er}(\beta)$. Here FP_1 and FP_2 refers to the pre and post false positive measures.

L	p	O	[A]				[H]				[E]				[NR]
			γ			β	γ			β	γ			β	β
			FN	FP ₁	FP ₂	Er	FN	FP ₁	FP ₂	Er	FN	FP ₁	FP ₂	Er	Er
0	100	10	0.00	1.78	1.13	1.11	0.30	0.74	0.62	1.09	0.00	12.13	3.07	1.17	1.51
0	100	20	0.00	1.10	0.67	1.14	0.46	0.30	0.47	1.13	0.00	15.54	3.48	1.19	1.91
0	100	30	0.00	1.00	0.57	1.07	1.63	0.00	0.32	1.11	0.00	16.92	4.12	1.09	2.29
0	100	40	0.36	0.38	0.33	1.16	4.33	0.00	0.00	1.32	0.00	14.80	2.69	1.19	2.59
0	300	10	0.00	2.53	1.18	0.51	0.00	2.72	1.18	0.52	0.00	11.15	2.68	0.54	0.81
0	300	20	0.00	1.41	0.93	0.55	0.41	1.10	0.59	0.54	0.00	11.73	2.71	0.56	1.03
0	300	30	0.28	0.98	0.41	0.62	1.68	0.35	0.32	0.59	0.00	10.57	1.91	0.59	1.19
0	300	40	1.29	0.25	0.27	0.73	3.61	0.00	0.00	0.69	0.17	9.88	1.83	0.65	1.19
1	100	10	0.00	1.17	0.96	1.10	0.00	0.90	0.62	1.10	0.91	11.35	1.97	1.21	1.77
1	100	20	0.26	0.45	0.49	1.00	0.99	0.24	0.37	1.02	3.81	10.31	2.54	1.74	1.93
1	100	30	1.23	0.43	0.47	1.31	3.66	0.00	0.00	1.29	8.89	10.13	2.37	1.80	2.12
1	100	40	14.35	0.47	0.55	1.73	14.92	0.36	0.43	1.82	13.48	9.87	1.96	1.90	2.49
1	300	10	0.00	2.36	0.97	0.52	0.00	2.29	1.01	0.52	1.77	7.94	2.41	0.59	0.87
1	300	20	0.00	1.14	0.54	0.52	0.58	0.40	0.39	0.49	6.28	8.99	2.44	0.96	0.93
1	300	30	5.35	0.36	0.36	0.73	1.85	0.00	0.42	0.61	12.82	6.83	1.89	0.96	0.91
1	300	40	14.66	0.00	0.36	0.86	11.92	0.00	0.00	0.77	18.51	6.93	2.18	0.94	0.94

1.2 HIV data analysis

1.2.1 *Robust HIV data analysis with $\mathbf{C} = \mathbf{1}_p$* Figure S1 – S3 shows the model fit diagnostic with RobRegCC in analyzing the HIV microbial abundance data to explore its association with the immune inflammation marker CD14.

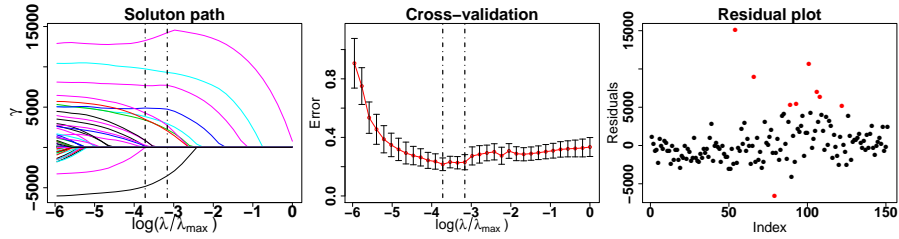


Figure S1. Robust HIV data analysis with adaptive elastic net penalty: For $\mathbf{C} = \mathbf{1}_p$, left and middle plot shows the solution path, representing mean shift parameter γ estimate, and cross-validation error with varying tuning parameter λ using **RobRegCC** model with adaptive Elastic-net penalty, respectively. Vertical dashed lines are corresponding to the minimum and one standard error rule test error. Identified outliers (red) are depicted using the residual plot (right).

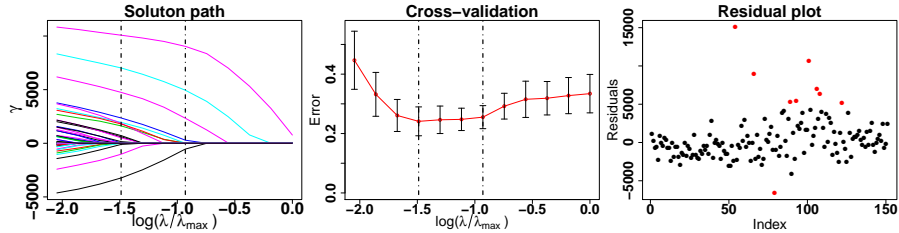


Figure S2. Robust HIV data analysis with elastic net penalty: For $\mathbf{C} = \mathbf{1}_p$, left and middle plot show solution path, representing mean shift parameter γ estimate, and cross-validation error with varying tuning parameter λ using **RobRegCC** model with Elastic-net penalty, respectively. Vertical dashed lines are corresponding to minimum and one standard error rule test error. Identified outliers (red) are depicted using the residual plot (right).

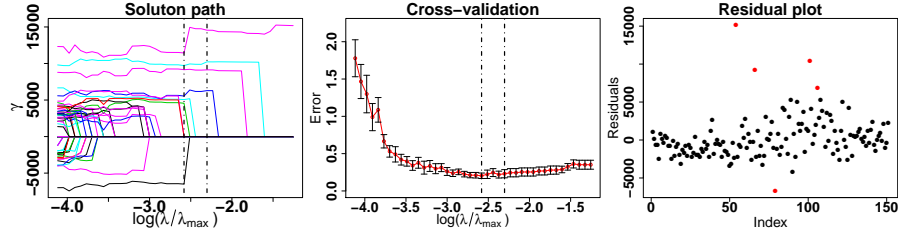


Figure S3. Robust HIV data analysis with hard ridge penalty: For $\mathbf{C} = \mathbf{1}_p$, left and middle plot show solution path, representing mean shift parameter γ estimate, and cross-validation error with varying tuning parameter λ using **RobRegCC** model with hard ridge penalty, respectively. Vertical dashed lines are corresponding to minimum and one standard error rule test error. Identified outliers (red) are depicted using the residual plot (right).

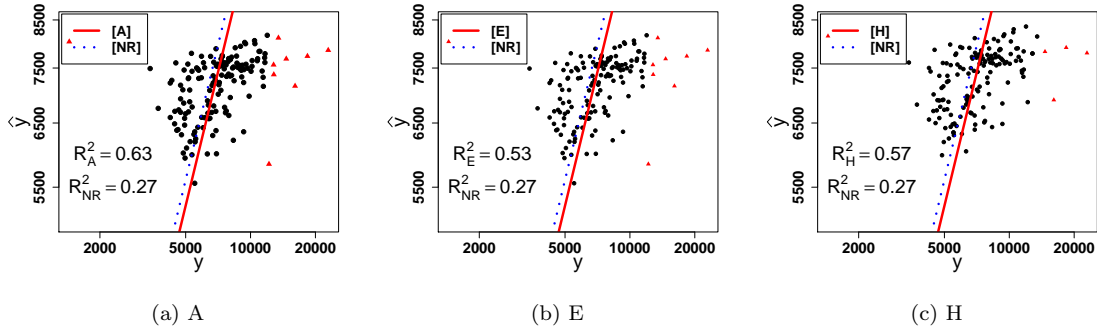


Figure S4. Application - Robust HIV data analysis for $\mathbf{C} = \mathbf{1}_p$: Comparison of the robust and non-robust approach in terms of the model fit statistics R^2 and outliers identified (red). In the robust procedure using RobRegCC, $R^2 = 1 - \|\epsilon_{\lambda_{cv}}\|^2 / \|\mathbf{y} - \bar{\mathbf{y}}\|^2$ where $\epsilon_{\lambda_{cv}} = \mathbf{y} - \mathbf{X}\hat{\boldsymbol{\theta}}_{\lambda_{cv}} - \hat{\gamma}_{\lambda_{cv}}$ and $\bar{\mathbf{y}}$ mean of \mathbf{y} .

1.2.2 *Robust HIV data analysis with $\mathbf{C} = \mathbf{1}_p$ after corrupting the responses \mathbf{y}* We corrupt $O = 10$ observations (see main manuscript for the procedure) in the response \mathbf{y} , denoting soluble CD14 marker. Figure S5 – S7 shows the model fit diagnostic with RobRegCC in analyzing the HIV microbial abundance data to explore its association with the immune inflammation marker CD14.

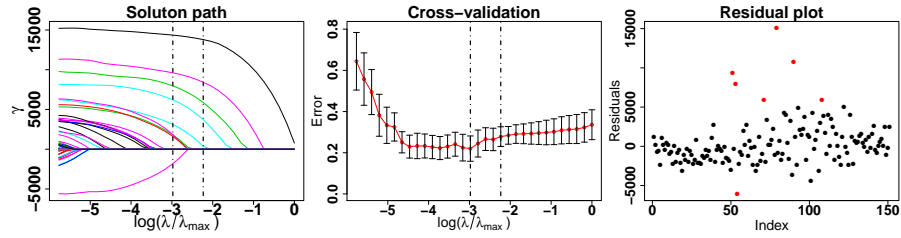


Figure S5. Robust HIV data analysis with adaptive elastic net penalty with corrupted response y : For $C = \mathbf{1}_p$, left and middle plot shows the solution path, representing mean shift parameter γ estimate, and cross-validation error with varying tuning parameter λ using **RobRegCC** model with adaptive Elastic-net penalty, respectively. Vertical dashed lines are corresponding to the minimum and one standard error rule test error. Identified outliers (red) are depicted using the residual plot (right).

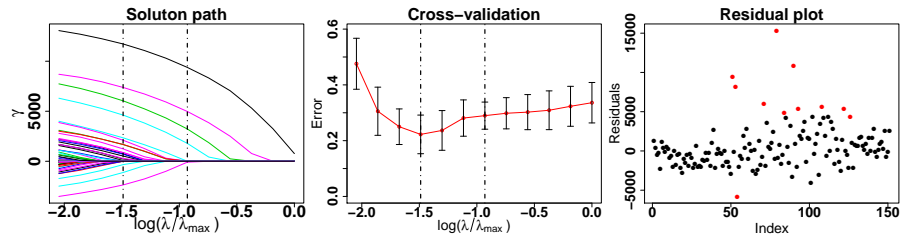


Figure S6. Robust HIV data analysis with elastic net penalty with corrupted response y : For $C = \mathbf{1}_p$, left and middle plot show solution path, representing mean shift parameter γ estimate, and cross-validation error with varying tuning parameter λ using **RobRegCC** model with Elastic-net penalty, respectively. Vertical dashed lines are corresponding to minimum and one standard error rule test error. Identified outliers (red) are depicted using the residual plot (right).

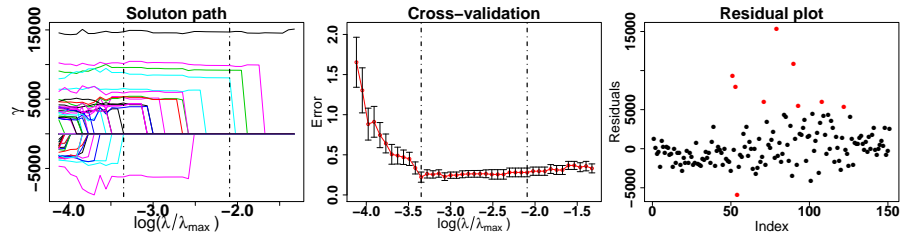


Figure S7. Robust HIV data analysis with hard ridge penalty with corrupted response y : For $C = \mathbf{1}_p$, left and middle plot show solution path, representing mean shift parameter γ estimate, and cross-validation error with varying tuning parameter λ using **RobRegCC** model with hard ridge penalty, respectively. Vertical dashed lines are corresponding to minimum and one standard error rule test error. Identified outliers (red) are depicted using the residual plot (right).

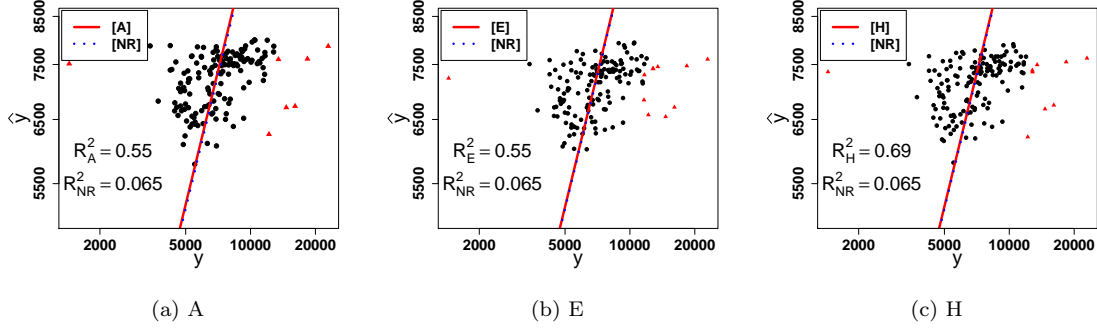


Figure S8. Application - Robust HIV data analysis for $\mathbf{C} = \mathbf{1}_p$: Comparison of the robust and non-robust approach in terms of the model fit statistics R^2 and outliers identified (red). In the robust procedure using RobRegCC, $R^2 = 1 - \|\epsilon_{\lambda_{cv}}\|^2 / \|\mathbf{y} - \bar{y}\|^2$ where $\epsilon_{\lambda_{cv}} = \mathbf{y} - \mathbf{X}\hat{\boldsymbol{\theta}}_{\lambda_{cv}} - \hat{\gamma}_{\lambda_{cv}}$ and \bar{y} mean of \mathbf{y} .

1.2.3 *Robust HIV data analysis with the phylum level subcomposition C* Figure S9 – S11 shows the model fit diagnostic with RobRegCC in analyzing the HIV microbial abundance data to explore its association with the immune inflammation marker CD14.

The subcomposition matrix for the robust analysis:

$$\mathbf{C}^T = \begin{bmatrix} \mathbf{1}_{p_1}^T & \mathbf{0} & \cdots & \mathbf{0} \\ \mathbf{0} & \mathbf{1}_{p_2}^T & \cdots & \mathbf{0} \\ \vdots & \vdots & \ddots & \vdots \\ \mathbf{0} & \mathbf{0} & \cdots & \mathbf{1}_{p_4}^T \end{bmatrix}_{6 \times 60} \quad (1.19)$$

with $\mathbf{s} = [0, 13, 35, 39, 45, 47, 60]$, $p_i = \mathbf{s}_{i+1} - \mathbf{s}_i$, $i = 1, \dots, 8$, and index sets $\mathbb{A}_i = \{\mathbf{s}_i + 1, \dots, \mathbf{s}_{i+1}\}$.

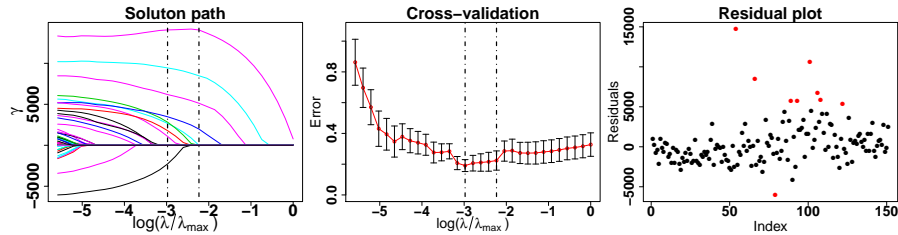


Figure S9. Robust HIV data analysis with adaptive elastic net penalty: For the subcomposition matrix \mathbf{C} due to order in the taxonomy, left and middle plot shows the solution path, representing mean shift parameter γ estimate, and cross-validation error with varying tuning parameter λ using **RobRegCC** model with adaptive Elastic-net penalty, respectively. Vertical dashed lines are corresponding to the minimum and one standard error rule test error. Identified outliers (red) are depicted using the residual plot (right).

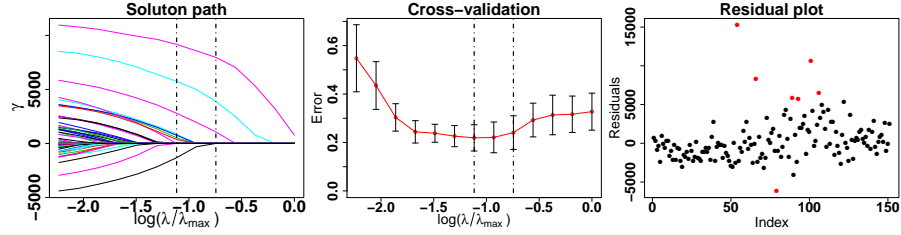


Figure S10. Robust HIV data analysis with elastic net penalty: For the subcomposition matrix \mathbf{C} due to order in the taxonomy, left and middle plot show solution path, representing mean shift parameter γ estimate, and cross-validation error with varying tuning parameter λ using **RobRegCC** model with Elastic-net penalty, respectively. Vertical dashed lines are corresponding to minimum and one standard error rule test error. Identified outliers (red) are depicted using the residual plot (right).

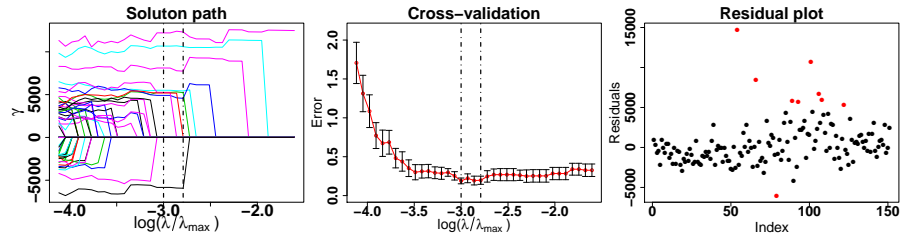


Figure S11. Robust HIV data analysis with hard ridge penalty: For the subcomposition matrix \mathbf{C} due to order in the taxonomy left and middle plot show solution path, representing mean shift parameter γ estimate, and cross-validation error with varying tuning parameter λ using **RobRegCC** model with hard ridge penalty, respectively. Vertical dashed lines are corresponding to minimum and one standard error rule test error. Identified outliers (red) are depicted using the residual plot (right).

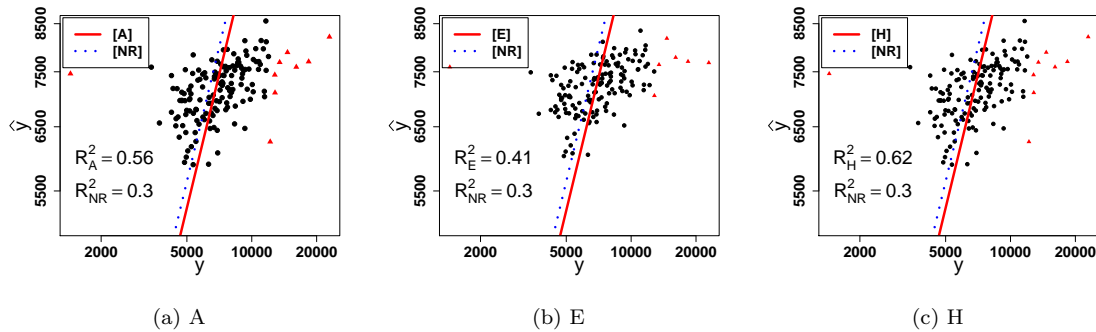


Figure S12. Application - Robust HIV data analysis for the subcomposition \mathbf{C} due to phylum in the taxonomy: Comparison of the robust and non-robust approach in terms of the model fit statistics R^2 and outliers identified (red). In the robust procedure using RobRegCC, $R^2 = 1 - \|\epsilon_{\lambda_{cv}}\|^2 / \|\mathbf{y} - \bar{y}\|^2$ where $\epsilon_{\lambda_{cv}} = \mathbf{y} - \mathbf{X}\hat{\theta}_{\lambda_{cv}} - \hat{\gamma}_{\lambda_{cv}}$ and \bar{y} mean of \mathbf{y} .

1.3 Details about the robust initialization

Here, we discuss the principal sensitive component (PSC) based analysis for the sparse log-contrast model (S-LCM) (Shi *and others*, 2016). Computing the sensitivity \mathbf{R} (3.13) for the least square estimator is trivial (Peña and Yohai, 1999) as it avoids the separate model fitting to obtain \hat{y}_i 's and $\hat{y}_{i(j)}$'s. Interestingly, the log-contrast model (LCM) follows the linear model. But the same is not true for the S-LCM, hence, computing \mathbf{R} is nontrivial. To overcome the challenge, we identify the support of the S-LCM coefficient estimate, and compute \mathbf{R} for the subsequent LCM (non-sparse). Please refer Algorithm 2 for the formula of calculating \mathbf{R} .

For the analysis, consider setting the parameter $\tau \in (0, 0.5)$ and obtain $m = n\tau$. Suppose $[\mathbf{u}_1, \dots, \mathbf{u}_q]$ denote the principal components of \mathbf{R} . Peña and Yohai (1999) characterized the extreme observations in terms of the value of entries in a principal component of \mathbf{R} . Following PENSE, for each \mathbf{u}_i , we generate three candidate subsamples by removing m observations corresponding to the: I) largest \mathbf{u}_i ; II) smallest \mathbf{u}_i ; III) largest $|\mathbf{u}_i|$. Including the one with all observations, the protocol results in total $3 * q + 1$ candidate samples. For each candidate sample, we estimate the coefficient of S-LCM using the default procedure specified in Shi *and others* (2016). Now, using the coefficient estimate, we evaluate the candidate samples in terms of the M-estimator of scale (Rousseeuw and Hubert, 2011) of the residuals obtained on full sample. Suppose the chosen candidate sample attains the minimum scale value s_1 . A potentially "clean subsample" is then obtained after discarding observations with the residuals magnitude (on the full data) greater than some $C's_1$. See Cohen Freue *and others* (2017) for the choice of C' .

The analysis may not detect the low-leveraged outliers. To solve, Peña and Yohai (1999) suggested to iterate the process several times or until convergence. Final S-LCM coefficient estimate on the clean subsample, and the residuals on full data, are used as initial estimator of the RobRegCC model, i.e., $\ddot{\delta} = [\ddot{\beta}^T \ddot{\gamma}^T]^T$. We have summarized the initialization procedure in the Algorithm 2.

Algorithm 2 Initialization via PSC analysis

Given $\mathbf{y}, \mathbf{Z}, \mathbf{h} = [h_1, \dots, h_n] = \text{diag}(\mathbf{P}\mathbf{Z})$, $\tau \in (0, 0.5)$, $C_1 = 2$.
Denote sorted \mathbf{h} by $[h_{(1)}, \dots, h_{(n)}]$.
Choose method: $\mathbf{M} = \{\text{S-LCM}, \text{LCM}\}$
Define index set $\mathcal{A}^{[0]} = \{i : h_i \leq h_{(n\alpha_1)}\}$, scale $s_0 = 1e^8$ with $\alpha \in (0.5, 1)$.
repeat
 $\{\mathcal{A}^{[i+1]}, s_{i+1}\} \leftarrow \text{PSC-Analysis}(\mathbf{y}, \mathbf{Z}, \mathcal{A}^{[i]}, \tau, C_1)$
until convergence, $|s_{i+1} - s_i| \leq 10^{-4}$.
return Index set \mathcal{A} .

Solution:
 $\tilde{\beta} \leftarrow \mathbf{M}(\mathbf{y}_{\mathcal{A}}, \mathbf{Z}_{\mathcal{A}})$; For more details of S-LCM see Shi *and others* (2016).
 $\tilde{\gamma} = \mathbf{y} - \mathbf{Z}\tilde{\beta}$
return $\tilde{\delta} = [\tilde{\beta}^T \tilde{\gamma}^T]^T$

PSC-Analysis($\mathbf{y}, \mathbf{Z}, \mathcal{A}, \tau, C_1$)

$\bar{\beta} \leftarrow \mathbf{M}(\mathbf{y}_{\mathcal{A}}, \mathbf{Z}_{\mathcal{A}})$, $\bar{\epsilon} \leftarrow \mathbf{y}_{\mathcal{A}} - \mathbf{Z}_{\mathcal{A}}\bar{\beta}$, $\mathcal{B} = \{i : \bar{\beta}_i \neq 0\}$, $n_1 = |\mathcal{A}|$, $m = n_1\tau$.

Denote subset matrix $\mathbf{Z}_{\mathcal{A}\mathcal{B}}$, projection matrix $\mathbf{H} = \mathbf{P}_{\mathbf{Z}_{\mathcal{A}\mathcal{B}}}$

Define \mathbf{W} as $\text{diag}(\mathbf{W}) = \bar{\epsilon}/(1 - \text{diag}(\mathbf{H}))$.

Compute $\mathbf{R} = \mathbf{H}\mathbf{W}^2\mathbf{H}$.

$\mathbf{U} = [\mathbf{u}_1, \dots, \mathbf{u}_q] \leftarrow$ Principal components of \mathbf{R} .

SOLUTION : $\tilde{\beta} = \bar{\beta}$, $\tilde{\gamma} = \bar{\epsilon}$ and scale $\tilde{s} = \text{M-estimator}(\bar{\epsilon})$.

for $i \in \{1, \dots, q\}$ **do**

$\{\mathcal{A}_1, \mathcal{A}_2, \mathcal{A}_3\} \leftarrow$ index set discarding m largest \mathbf{u}_i , smallest \mathbf{u}_i , and largest $|\mathbf{u}_i|$.

for $j \in \{1, 2, 3\}$ **do**

$\bar{\beta} \leftarrow \mathbf{M}(\mathbf{y}_{\mathcal{A}_j}, \mathbf{Z}_{\mathcal{A}_j})$, $\bar{\epsilon} \leftarrow \mathbf{y}_{\mathcal{A}_j} - \mathbf{Z}_{\mathcal{A}_j}\bar{\beta}$

if (M-estimator($\bar{\epsilon}$) < \tilde{s}) **then**

 SOLUTION : $\tilde{\beta} = \bar{\beta}$, $\tilde{\gamma} = \bar{\epsilon}$ and scale $\tilde{s} = \text{M-estimator}(\bar{\epsilon})$.

end if

end for

end for

return $\{|\mathbf{y} - \mathbf{Z}\tilde{\beta}| < C_1\tilde{s}, \tilde{s}\}$.

1.4 Non-asymptotic analysis proofs

Proof of Theorem 4.1. We consider the following optimization problem for the non-asymptotic analysis:

$$\{\hat{\gamma}_{\lambda_1}, \hat{\beta}_{\lambda_2}\} \equiv \arg \min_{\{\gamma, \beta\}} f_{\lambda_1, \lambda_2}(\beta, \gamma; \mathbf{Z}, \mathbf{y}) \quad \text{s.t.} \quad \mathbf{C}^T \beta = \mathbf{0},$$

where $f_{\lambda_1, \lambda_2}(\beta, \gamma; \mathbf{Z}, \mathbf{y}) = \frac{1}{2} \|\mathbf{y} - \mathbf{Z}\beta - \gamma\|_2^2 + P_{\lambda_1}^1(\gamma) + P_{\lambda_2}^2(\beta)$. For the ease of presentation, we

drop the subscript $\{\lambda_1, \lambda_2\}$ from $f_{\lambda_1, \lambda_2}(\cdot)$ and $\{\hat{\gamma}_{\lambda_1}, \hat{\beta}_{\lambda_2}\}$. Then, for the optimal solution $\{\hat{\beta}, \hat{\gamma}\}$,

we have

$$f(\widehat{\beta}_\lambda, \widehat{\gamma}_\lambda; \mathbf{Z}, \mathbf{y}) \leq f(\beta, \gamma; \mathbf{Z}, \mathbf{y}),$$

where $\{\beta, \gamma\} \in \mathbb{R}^{p+n}$ such that $\mathbf{C}^T \beta = \mathbf{0}$. On simplification, we write the basic inequality in terms of the true model parameters $\{\beta^*, \gamma^*\}$, specified in equation (4.15), as

$$\begin{aligned} M(\widehat{\beta}_\lambda - \beta^*, \widehat{\gamma}_\lambda - \gamma^*) &\leq M(\beta - \beta^*, \gamma - \gamma^*) + 2\langle \epsilon, \mathbf{Z}\Delta^{(\beta)} + \Delta^{(\gamma)} \rangle \\ &\quad + P_{\lambda_1}^1(\gamma) - P_{\lambda_1}^1(\widehat{\gamma}) + P_{\lambda_2}^2(\beta) - P_{\lambda_2}^2(\widehat{\beta}), \end{aligned} \quad (1.20)$$

where $\Delta^{(\beta)} = \widehat{\beta} - \beta$ and $\Delta^{(\gamma)} = \widehat{\gamma} - \gamma$. To simplify further, we use following lemma to bound the stochastic term $\langle \epsilon, \mathbf{Z}\Delta^{(\beta)} + \Delta^{(\gamma)} \rangle$.

LEMMA 1.1 Define hard threshold penalty $P_\lambda^h(u) = (-u^2/2 + \lambda|u|)1_{|u| < \lambda} + (u^2/2)1_{|u| \geq \lambda}$. Consider $\mathbf{U} \in \mathbb{R}^{n \times p}$, $\mathbf{C} \in \mathbb{R}^{p \times k}$ and define $\Gamma_{T,S} = \{(\gamma, \beta) \in \mathbb{R}^n \otimes \mathbb{R}^p; \mathbf{T} = \mathcal{J}(\gamma), \mathbf{S} = \mathcal{J}(\beta), \mathbf{C}^T \beta = \mathbf{0}\}$ where operator $\mathcal{J}(\cdot)$ denote support index set with $s = |\mathbf{S}|$ such that $1 < s < p$ and $t = |\mathbf{T}|$ such that $1 < t < n$. Suppose tuning parameter $\lambda_1 = A\lambda_a$ and $\lambda_2 = A\lambda_b$ with $\lambda_a = \sigma\sqrt{\log en}$, $\lambda_b = \sigma\sqrt{\log ep}$, and $A = \sqrt{ab}A_1$ for a sufficiently large A_1 satisfying $a \geq 2b > 0$. There exist constant L, C', c and parameter v , we have

$$\sup_{(\beta, \gamma) \in \Gamma_{T,S}} \left\{ 2\langle \epsilon, \mathbf{U}\beta + \gamma \rangle - \frac{1}{a} \|\mathbf{U}\beta + \gamma\|_2^2 - \frac{P_{\lambda_1}^h(\gamma)}{b} - \frac{P_{\lambda_2}^h(\beta)}{b} - 2aL\sigma^2(2-k) \right\} \geq a\sigma^2v$$

with probability at most $C' \exp(-cv)$.

Using the lemma, we bound the stochastic component of the basic inequality (1.20) as

$$\begin{aligned} 2\langle \epsilon, \mathbf{Z}\Delta^{(\beta)} + \Delta^{(\gamma)} \rangle &\leq \frac{1}{a} \|\mathbf{Z}\Delta^{(\beta)} + \Delta^{(\gamma)}\|_2^2 + \frac{1}{b} P_{\lambda_1}^h(\Delta^{(\gamma)}) + \frac{1}{b} P_{\lambda_2}^h(\Delta^{(\beta)}) + \\ &\quad R + 2aL\sigma^2(2-k), \end{aligned}$$

where $\frac{1}{a}\|\mathbf{Z}\Delta^{(\beta)} + \Delta^{(\gamma)}\|_2^2 \leq \frac{2M(\boldsymbol{\beta}-\boldsymbol{\beta}^*, \boldsymbol{\gamma}-\boldsymbol{\gamma}^*)}{a} + \frac{2M(\widehat{\boldsymbol{\beta}}-\boldsymbol{\beta}^*, \widehat{\boldsymbol{\gamma}}-\boldsymbol{\gamma}^*)}{a}$ and

$$R = \sup_{\substack{1 \leq s \leq p \\ 1 \leq t \leq n}} \sup_{(\boldsymbol{\beta}, \boldsymbol{\gamma}) \in \Gamma_{T,S}} \left\{ 2\langle \boldsymbol{\epsilon}, \mathbf{Z}\Delta^{(\beta)} + \Delta^{(\gamma)} \rangle - \frac{1}{a}\|\mathbf{Z}\Delta^{(\beta)} + \Delta^{(\gamma)}\|_2^2 - \frac{1}{b}P_{\lambda_1}^h(\Delta^{(\gamma)}) - \frac{1}{b}P_{\lambda_2}^h(\Delta^{(\beta)}) \right\}$$

with expectation $\mathbb{E}(R) \leq ac\sigma^2$. Using the result, we write the basic inequality (1.20) as

$$\begin{aligned} \left(1 - \frac{1}{a}\right)M(\widehat{\boldsymbol{\beta}} - \boldsymbol{\beta}^*, \widehat{\boldsymbol{\gamma}} - \boldsymbol{\gamma}^*) &\leq \left(1 + \frac{1}{a}\right)M(\boldsymbol{\beta} - \boldsymbol{\beta}^*, \boldsymbol{\gamma} - \boldsymbol{\gamma}^*) + \\ &\frac{1}{b}P_{\lambda_1}^h(\Delta^{(\gamma)}) + \frac{1}{b}P_{\lambda_2}^h(\Delta^{(\beta)}) + 2aL\sigma^2(2-k) + R + \\ &P_{\lambda_1}^1(\boldsymbol{\gamma}) - P_{\lambda_1}^1(\widehat{\boldsymbol{\gamma}}) + P_{\lambda_2}^2(\boldsymbol{\beta}) - P_{\lambda_2}^2(\widehat{\boldsymbol{\beta}}). \end{aligned} \quad (1.21)$$

To simplify further, we use the inequality $P_{\lambda_1}^h(\Delta^{(\gamma)}) \leq P_{\lambda_1}^h(\boldsymbol{\gamma}) + P_{\lambda_1}^h(\widehat{\boldsymbol{\gamma}})$ and $P_{\lambda_1}^h(\boldsymbol{\gamma}) \leq P_{\lambda_1}^1(\boldsymbol{\gamma})$, and write

$$\begin{aligned} P_{\lambda_1}^1(\boldsymbol{\gamma}) - P_{\lambda_1}^1(\widehat{\boldsymbol{\gamma}}) + \frac{1}{b}P_{\lambda_1}^h(\Delta^{(\gamma)}) &\leq \left(1 + \frac{1}{b}\right)P_{\lambda_1}^1(\boldsymbol{\gamma}) + \left(\frac{1}{b} - 1\right)P_{\lambda_1}^1(\widehat{\boldsymbol{\gamma}}) \\ &\leq \left(1 + \frac{1}{b}\right)P_{\lambda_1}^1(\boldsymbol{\gamma}). \end{aligned}$$

Similarly, we simplify $P_{\lambda_2}^2(\boldsymbol{\beta}) - P_{\lambda_2}^2(\widehat{\boldsymbol{\beta}}) + \frac{1}{b}P_{\lambda_2}^h(\Delta^{(\beta)}) \leq \left(1 + \frac{1}{b}\right)P_{\lambda_2}^2(\boldsymbol{\beta})$. Now, we use the result from (1.21) and write the expression for the prediction error bound as

$$\begin{aligned} \left(1 - \frac{1}{a}\right)M(\widehat{\boldsymbol{\beta}} - \boldsymbol{\beta}^*, \widehat{\boldsymbol{\gamma}} - \boldsymbol{\gamma}^*) &\leq \left(1 + \frac{1}{a}\right)M(\boldsymbol{\beta} - \boldsymbol{\beta}^*, \boldsymbol{\gamma} - \boldsymbol{\gamma}^*) + R + \\ &\left(1 + \frac{1}{b}\right)\{P_{\lambda_1}^1(\boldsymbol{\gamma}) + P_{\lambda_2}^2(\boldsymbol{\beta})\} + 2aL\sigma^2(2-k). \end{aligned}$$

Thus, the oracle bound on the prediction error is

$$M(\widehat{\boldsymbol{\beta}} - \boldsymbol{\beta}^*, \widehat{\boldsymbol{\gamma}} - \boldsymbol{\gamma}^*) \lesssim M(\boldsymbol{\beta} - \boldsymbol{\beta}^*, \boldsymbol{\gamma} - \boldsymbol{\gamma}^*) + P_{\lambda_1}^1(\boldsymbol{\gamma}) + P_{\lambda_2}^2(\boldsymbol{\beta}) + \sigma^2(3-k),$$

where \lesssim means the inequality holds upto a multiplicative constant. □

Proof of Theorem 4.5. We follow the proof of Theorem 4.1 to prove the result. The result corresponds to the case II with LASSO penalty, i.e., $P_{\lambda_1}^1(\boldsymbol{\gamma}) = \lambda_1|\boldsymbol{\gamma}|_1$ and $P_{\lambda_2}^2(\boldsymbol{\beta}) = \lambda_2|\boldsymbol{\beta}|_1$. Note

that $P_{\lambda_1}^h(\Delta^{(\gamma)}) \leq \lambda_1 |\Delta^{(\gamma)}|_1$ and $P_{\lambda_2}^h(\Delta^{(\beta)}) \leq \lambda_2 |\Delta^{(\beta)}|_1$. Now, consider $\theta = 1/b$ and simplify

$$\begin{aligned}
P_{\lambda_1}^1(\gamma) - P_{\lambda_1}^1(\hat{\gamma}) + \frac{P_{\lambda_1}^h(\Delta^{(\gamma)})}{b} &\leq P_{\lambda_1}^1(\gamma) - P_{\lambda_1}^1(\hat{\gamma}) + \frac{\lambda_1 |\Delta^{(\gamma)}|_1}{b} \\
&= \lambda_1 \left\{ |\gamma|_1 - |\hat{\gamma}|_1 + \theta |\Delta^{(\gamma)}|_1 \right\} \\
&\leq \lambda_1 \left\{ |\Delta_{\mathbf{T}}^{(\gamma)}|_1 - |\Delta_{\mathbf{T}^c}^{(\gamma)}|_1 + \theta |\Delta_{\mathbf{T}}^{(\gamma)}|_1 + \theta |\Delta_{\mathbf{T}^c}^{(\gamma)}|_1 \right\} \\
&\leq \lambda_1 \left\{ (1 + \theta) |\Delta_{\mathbf{T}}^{(\gamma)}|_1 - (1 - \theta) |\Delta_{\mathbf{T}^c}^{(\gamma)}|_1 \right\} \\
&= \lambda_1 (1 - \theta) \left\{ (1 + \nu) |\Delta_{\mathbf{T}}^{(\gamma)}|_1 - |\Delta_{\mathbf{T}^c}^{(\gamma)}|_1 \right\}
\end{aligned}$$

where $\theta = \nu/(1 + \nu)$. Similarly,

$$P_{\lambda_2}^2(\beta) - P_{\lambda_2}^2(\hat{\beta}) + \frac{P_{\lambda_2}^h(\Delta^{(\beta)})}{b} \leq \lambda_2 (1 - \theta) \left\{ (1 + \nu) |\Delta_{\mathbf{S}}^{(\beta)}|_1 - |\Delta_{\mathbf{S}^c}^{(\beta)}|_1 \right\}.$$

On combining the two results, we get

$$\begin{aligned}
P_{\lambda_2}^2(\beta) - P_{\lambda_2}^2(\hat{\beta}) + \frac{P_{\lambda_2}^h(\Delta^{(\beta)})}{b} + P_{\lambda_1}^1(\gamma) - P_{\lambda_1}^1(\hat{\gamma}) + \frac{P_{\lambda_1}^h(\Delta^{(\gamma)})}{b} &\leq \\
\lambda_2 (1 - \theta) \left\{ (1 + \nu) |\Delta_{\mathbf{S}}^{(\beta)}|_1 - |\Delta_{\mathbf{S}^c}^{(\beta)}|_1 \right\} + \lambda_1 (1 - \theta) \left\{ (1 + \nu) |\Delta_{\mathbf{T}}^{(\gamma)}|_1 - |\Delta_{\mathbf{T}^c}^{(\gamma)}|_1 \right\}. &
\end{aligned}$$

Under the compatibility condition on RHS, we further simplify

$$\begin{aligned}
\frac{\text{RHS}}{1 - \theta} &\leq \lambda_1 \kappa_1 t^{1/2} \|\mathbf{P}_{\mathbf{Z}\Delta^{(\beta)}}^\perp(\mathbf{Z}\Delta^{(\beta)} + \Delta^{(\gamma)})\|_2 + \lambda_2 \kappa_2 s^{1/2} \|\mathbf{P}_{\mathbf{Z}\Delta^{(\beta)}}(\mathbf{Z}\Delta^{(\beta)} + \Delta^{(\gamma)})\|_2 \\
\text{RHS} &\leq \lambda_1 (1 - \theta) \kappa_1 t^{1/2} \|\mathbf{Z}\Delta^{(\beta)} + \Delta^{(\gamma)}\|_2 + \lambda_2 (1 - \theta) \kappa_2 s^{1/2} \|\mathbf{Z}\Delta^{(\beta)} + \Delta^{(\gamma)}\|_2 \\
&\leq \frac{2}{a} \|\mathbf{Z}\Delta^{(\beta)} + \Delta^{(\gamma)}\|_2^2 + a \lambda_1^2 (1 - \theta)^2 \kappa_1^2 t + a \lambda_2^2 (1 - \theta)^2 \kappa_2^2 s
\end{aligned}$$

Using the upper bound $\|\mathbf{Z}\Delta^{(\beta)} + \Delta^{(\gamma)}\|_2^2 \leq M(\hat{\beta} - \beta^*, \hat{\gamma} - \gamma^*) + M(\beta - \beta^*, \gamma - \gamma^*)$, and following the proof of Theorem 4.1, we write

$$\begin{aligned}
\left(1 - \frac{2}{a}\right) M(\hat{\beta} - \beta^*, \hat{\gamma} - \gamma^*) &\leq \left(1 + \frac{2}{a}\right) M(\beta - \beta^*, \gamma - \gamma^*) + 2aL\sigma^2(2 - k) \\
&\quad + a\lambda_1^2(1 - \theta)^2 \kappa_1^2 t + a\lambda_2^2(1 - \theta)^2 \kappa_2^2 s + R.
\end{aligned}$$

Thus, we can say that

$$M(\hat{\beta} - \beta^*, \hat{\gamma} - \gamma^*) \lesssim M(\beta - \beta^*, \gamma - \gamma^*) + a(1 - \theta)^2 \{\lambda_1^2 \kappa_1^2 t + \lambda_2^2 \kappa_2^2 s\} + (3 - k)\sigma^2.$$

□

Proof of lemma 1.1. We follows the approach from She (2016); She and Chen (2017); She (2017) to prove the result. We write the forms of hard threshold penalty as $P_\lambda^h(u) = (-u^2/2 + \lambda|u|)1_{|u| < \lambda} + (u^2/2)1_{|u| \geq \lambda}$ and $P_\lambda^0(u) = (u^2/2)1_{u \neq 0}$. Define

$$\begin{aligned} L_h(\boldsymbol{\beta}, \boldsymbol{\gamma}) &= 2\langle \boldsymbol{\epsilon}, \mathbf{U}\boldsymbol{\beta} + \boldsymbol{\gamma} \rangle - \frac{\|\mathbf{U}\boldsymbol{\beta} + \boldsymbol{\gamma}\|_2^2}{a} - \frac{P_{\lambda_1}^h(\boldsymbol{\gamma})}{b} - \frac{P_{\lambda_2}^h(\boldsymbol{\beta})}{b} - 2aL\sigma^2(2-k) \\ L_0(\boldsymbol{\beta}, \boldsymbol{\gamma}) &= 2\langle \boldsymbol{\epsilon}, \mathbf{U}\boldsymbol{\beta} + \boldsymbol{\gamma} \rangle - \frac{\|\mathbf{U}\boldsymbol{\beta} + \boldsymbol{\gamma}\|_2^2}{a} - \frac{P_{\lambda_1}^0(\boldsymbol{\gamma})}{b} - \frac{P_{\lambda_2}^0(\boldsymbol{\beta})}{b} - 2aL\sigma^2(2-k). \end{aligned}$$

The formulation implies $P_\lambda^h(\boldsymbol{\gamma}) \leq P_\lambda^0(\boldsymbol{\gamma})$ resulting in $L_h(\boldsymbol{\beta}, \boldsymbol{\gamma}) \geq L_0(\boldsymbol{\beta}, \boldsymbol{\gamma})$. Define set

$$\mathcal{A}_h = \left\{ \sup_{(\boldsymbol{\beta}, \boldsymbol{\gamma}) \in \Gamma_{T,S}} L_h(\boldsymbol{\beta}, \boldsymbol{\gamma}) \geq a\sigma^2v \right\}, \quad \mathcal{A}_0 = \left\{ \sup_{(\boldsymbol{\beta}, \boldsymbol{\gamma}) \in \Gamma_{T,S}} L_0(\boldsymbol{\beta}, \boldsymbol{\gamma}) \geq a\sigma^2v \right\}.$$

For any $\zeta \in \mathcal{A}_0$, the formulation implies $\zeta \in \mathcal{A}_H$, hence, $\mathcal{A}_0 \subseteq \mathcal{A}_H$. To prove $\mathcal{A}_0 = \mathcal{A}_H$, we aim to prove $\mathcal{A}_H \subseteq \mathcal{A}_0$. It should be noted that

$$\mathcal{A}_h \subset \left\{ \sup_{(\boldsymbol{\beta}, \boldsymbol{\gamma})} L_h(\boldsymbol{\beta}, \boldsymbol{\gamma}) \geq a\sigma^2v \right\}.$$

The occurrence of \mathcal{A}_h implies that $L_h(\boldsymbol{\beta}^0, \boldsymbol{\gamma}^0) \geq a\sigma^2v$ for any $(\boldsymbol{\beta}^0, \boldsymbol{\gamma}^0)$ satisfying

$$(\boldsymbol{\beta}^0, \boldsymbol{\gamma}^0) \equiv \arg \min_{(\boldsymbol{\beta}, \boldsymbol{\gamma})} \frac{\|\mathbf{U}\boldsymbol{\beta} + \boldsymbol{\gamma}\|_2^2}{a} - 2\langle \boldsymbol{\epsilon}, \mathbf{U}\boldsymbol{\beta} + \boldsymbol{\gamma} \rangle + \frac{P_{\lambda_1}^h(\boldsymbol{\gamma})}{b} + \frac{P_{\lambda_2}^h(\boldsymbol{\beta})}{b}$$

LEMMA 1.2 (For proof see She (2012)) Suppose $\alpha > 1$. For $\mathbf{y} \in \mathbb{R}^n$, there exist a globally optimal solution $\boldsymbol{\gamma}^0$ satisfying

$$\boldsymbol{\gamma}^0 \equiv \arg \min_{\boldsymbol{\gamma}} \frac{1}{2}\|\mathbf{y} - \boldsymbol{\gamma}\|_2^2 + \alpha P_\lambda^h(\boldsymbol{\gamma}),$$

such that for any $j : 1 \leq j \leq n$ either $\gamma_j^0 = 0$ or $|\gamma_j^0| \geq \lambda\alpha^{1/2} \geq \lambda$.

Lemma 1.2 and Lemma 5 from She (2016) indicate that a globally optimal solution $(\boldsymbol{\beta}^0, \boldsymbol{\gamma}^0)$ exist. Also, in a case with $a > 2b > 0$, we have $P_0(\boldsymbol{\gamma}; \lambda_1) + P_0(\boldsymbol{\beta}; \lambda_2) = P_h(\boldsymbol{\gamma}; \lambda_1) + P_h(\boldsymbol{\beta}; \lambda_2)$, and thus $L_0(\boldsymbol{\beta}^0, \boldsymbol{\gamma}^0) = L_h(\boldsymbol{\beta}^0, \boldsymbol{\gamma}^0)$. Moreover,

$$\sup_{(\boldsymbol{\beta}, \boldsymbol{\gamma}) \in \Gamma_{T,S}} L_0(\boldsymbol{\beta}, \boldsymbol{\gamma}) \geq L_0(\boldsymbol{\beta}^0, \boldsymbol{\gamma}^0) = L_h(\boldsymbol{\beta}^0, \boldsymbol{\gamma}^0) \geq a\sigma^2v,$$

suggests $\mathcal{A}_h \subseteq \mathcal{A}_0$. Hence, $\mathcal{A}_h = \mathcal{A}_0$. It is then sufficient to prove that

$$\mathbf{P}(\mathcal{A}_h) = \mathbf{P}(\mathcal{A}_0) \leq C' \exp(-cv).$$

Now, let \mathbf{I}_n be the identity matrix of size $n \times n$, and $\mathbf{I}_{\mathbf{S}}$ be the sub-matrix corresponding to columns in the index set \mathbf{S} . $\mathbf{P}_{\mathbf{I}_{\mathbf{S}}}$ denote the projection matrix for the sub-matrix $\mathbf{I}_{\mathbf{S}}$. Then, $\mathbf{P}_{\mathbf{I}_{\mathbf{S}}} + \mathbf{P}_{\mathbf{I}_{\mathbf{S}}}^{\mathbf{T}} = \mathbf{I}_n$. In terms of the projection matrix, we factorize the stochastic component

$$\langle \boldsymbol{\epsilon}, \mathbf{U}\boldsymbol{\beta} + \boldsymbol{\gamma} \rangle = \langle \boldsymbol{\epsilon}, \mathbf{P}_{\mathbf{I}_{\mathbf{S}}}^{\mathbf{T}} \mathbf{U}\boldsymbol{\beta} \rangle + \langle \boldsymbol{\epsilon}, \mathbf{P}_{\mathbf{I}_{\mathbf{S}}} (\mathbf{U}\boldsymbol{\beta} + \boldsymbol{\gamma}) \rangle = \langle \boldsymbol{\epsilon}, \mathbf{a}_1 \rangle + \langle \boldsymbol{\epsilon}, \mathbf{a}_2 \rangle,$$

where $\|\mathbf{a}_1\|_2^2 + \|\mathbf{a}_2\|_2^2 = \|\mathbf{U}\boldsymbol{\beta} + \boldsymbol{\gamma}\|_2^2$.

LEMMA 1.3 Given $\mathbf{U} \in \mathbb{R}^{n \times p}$, $\mathbf{C} \in \mathbb{R}^{p \times k}$, index set \mathbf{S} with $s = |\mathbf{S}|$ such that $1 < s < p$, and index set \mathbf{T} with $t = |\mathbf{T}|$ such that $1 < t < n$. Define set $\Gamma'_{\mathbf{T}, \mathbf{S}} = \{\boldsymbol{\alpha} \in \mathbb{R}^n; \|\boldsymbol{\alpha}\|_2 \leq 1, \boldsymbol{\alpha} = \mathbf{U}\boldsymbol{\beta}, \boldsymbol{\beta} \in \mathbb{R}^p, \boldsymbol{\alpha} \in \text{CS}(\mathbf{U}_{\mathbf{T}^c \mathbf{S}}), \mathbf{T} = \mathcal{J}(\boldsymbol{\gamma}), \mathbf{S} = \mathcal{J}(\boldsymbol{\beta}), \mathbf{C}^{\mathbf{T}}\boldsymbol{\beta} = \mathbf{0}\}$ where operator $\mathcal{J}(\cdot)$ denote the support set. Define $p'_1(t, s) = \sigma^2 \{s - k + \log \binom{n}{t} + \log \binom{p}{k} + \log \binom{p-k}{s-k}\}$. Then

$$\mathbf{P} \left(\sup_{\boldsymbol{\alpha} \in \Gamma'_{\mathbf{T}, \mathbf{S}}} \langle \boldsymbol{\epsilon}, \boldsymbol{\alpha} \rangle \geq v\sigma + \sqrt{Lp'_1(t, s)} \right) \leq C' \exp(-cv^2),$$

for sufficiently large constant $\{L, C', c\}$.

Proof of Lemma 1.3 follows from the Lemma 6 of She (2016) and the Lemma 4 of She (2017).

Now, using the lemma 1.3, we simplify the first term involving \mathbf{a}_1 . Thus, write

$$\begin{aligned} 2\langle \boldsymbol{\epsilon}, \mathbf{a}_1 \rangle - \frac{1}{a} \|\mathbf{a}_1\|^2 - 2aLp'_1(t, s) &= 2\langle \boldsymbol{\epsilon}, \mathbf{a}_1 \rangle - \frac{\|\mathbf{a}_1\|^2}{2a} - \frac{\|\mathbf{a}_1\|^2}{2a} - 2aLp'_1(t, s) \\ &\leq 2\langle \boldsymbol{\epsilon}, \frac{\mathbf{a}_1}{\|\mathbf{a}_1\|} \rangle \|\mathbf{a}_1\| - \frac{\|\mathbf{a}_1\|^2}{2a} - 2\|\mathbf{a}_1\| \{Lp'_1(t, s)\}^{1/2}, \end{aligned}$$

on applying the Cauchy-Schwarz inequality on the last two terms. Further, simplify RHS as

$$\begin{aligned} \text{RHS} &= 2\|\mathbf{a}_1\| \left(\langle \boldsymbol{\epsilon}, \frac{\mathbf{a}_1}{\|\mathbf{a}_1\|} \rangle - (Lp'_1(t, s))^{1/2} \right) - \frac{1}{2a} \|\mathbf{a}_1\|^2 \\ &\leq 2a \left(\langle \boldsymbol{\epsilon}, \frac{\mathbf{a}_1}{\|\mathbf{a}_1\|} \rangle - (Lp'_1(t, s))^{1/2} \right)_+^2 + \frac{1}{2a} \|\mathbf{a}_1\|^2 - \frac{1}{2a} \|\mathbf{a}_1\|^2 \\ &= 2a \left(\langle \boldsymbol{\epsilon}, \frac{\mathbf{a}_1}{\|\mathbf{a}_1\|_2} \rangle - (Lp'_1(t, s))^{1/2} \right)_+^2 \end{aligned}$$

Again, using the result from lemma 1.3, we have

$$\begin{aligned} & \mathbf{P} \left\{ \sup_{(\beta, \gamma) \in \Gamma_{T, s}} \left(2\langle \epsilon, \mathbf{a}_1 \rangle - \frac{\|\mathbf{a}_1\|^2}{a} - 2aLp'_1(t, s) \right) \geq \frac{1}{2}a\sigma^2v \right\} \leq \\ & \mathbf{P} \left\{ \sup_{(\beta, \gamma) \in \Gamma_{T, s}} 2a \left(\langle \epsilon, \frac{\mathbf{a}_1}{\|\mathbf{a}_1\|} \rangle - \{Lp'_1(t, s)\}^{1/2} \right)_+^2 \geq \frac{1}{2}a\sigma^2v \right\} \leq C' \exp(-cv). \end{aligned} \quad (1.22)$$

Similarly for \mathbf{a}_2 , we have

$$\mathbf{P} \left\{ \sup_{(\beta, \gamma) \in \Gamma_{T, s}} \left(2\langle \epsilon, \mathbf{a}_2 \rangle - \frac{1}{a}\|\mathbf{a}_2\|^2 - 2aLp'_2(t, s) \right) \geq \frac{1}{2}a\sigma^2v \right\} \leq C' \exp(-cv), \quad (1.23)$$

for $p'_2(t, s) = \sigma^2\{t + \log\binom{n}{t}\}$. On applying the union bound on the results obtained in (1.22) and (1.23), we have

$$\begin{aligned} & \mathbf{P} \left\{ \sup_{(\beta, \gamma) \in \Gamma_{T, s}} \left[2\langle \epsilon, \mathbf{U}\beta + \gamma \rangle - \frac{\|\mathbf{U}\beta + \gamma\|_2^2}{a} - 2aL\sigma^2 \left\{ s - k + t + 2\log\binom{n}{t} + \right. \right. \right. \\ & \left. \left. \left. \log\binom{p}{k} + \log\binom{p-k}{s-k} \right\} \right] \geq a\sigma^2v \right\} \\ & \leq C' \exp(-cv), \end{aligned} \quad (1.24)$$

for some constants $\{L, C', c\}$. Now, for the sufficiently large constant A_1 and $a \geq 2b > 0$, we can say that

$$2aL\sigma^2 \left\{ t + 2\log\binom{n}{t} \right\} \leq 2aL\sigma^2 \left\{ t + 2t\log\frac{en}{t} \right\} \leq 4aL\sigma^2 t \log(en) \leq \frac{P_{\lambda_1}^h(\gamma)}{b}.$$

Similarly,

$$\begin{aligned} s - k + \log\binom{p}{k} + \log\binom{p-k}{s-k} & \leq s - k + k\log\frac{ep}{k} + (s-k)\log\frac{ep}{s-k} \\ & = s\log ep + (s-k) - (s-k)\log(s-k) - k\log k \\ & \leq s\log ep + (s-k) - (s-k)\left(1 - \frac{1}{s-k}\right) - k\left(1 - \frac{1}{k}\right) \\ & = s\log ep + 2 - k, \end{aligned}$$

where second inequality is due to $1 - 1/m \leq \log m$. Thus, for sufficiently large A_1 , we write

$$\begin{aligned} 2aL\sigma^2 \left\{ s - k + \log\binom{p}{k} + \log\binom{p-k}{s-k} \right\} & \leq 2aL\sigma^2 (s\log ep + 2 - k) \\ & \leq \frac{1}{b}P_h(\beta; \lambda_2) + 2aL\sigma^2(2 - k). \end{aligned}$$

On applying the above inequality results in the union bound (1.24), we prove that

$$\mathbf{P} \left(\sup_{(\boldsymbol{\beta}, \boldsymbol{\gamma}) \in \Gamma_{T,S}} \left\{ 2 \langle \boldsymbol{\epsilon}, \mathbf{X}\boldsymbol{\beta} + \boldsymbol{\gamma} \rangle - \frac{1}{a} \|\mathbf{X}\boldsymbol{\beta} + \boldsymbol{\gamma}\|_2^2 - \frac{P_{\lambda_1}^h(\boldsymbol{\gamma})}{b} - \frac{P_{\lambda_2}^h(\boldsymbol{\beta})}{b} - 2aL\sigma^2(2-k) \right\} \geq a\sigma^2v \right) \leq C' \exp(-cv).$$

□